

國立臺灣大學公共衛生學院環境與職業健康科學研究所

碩士論文

Institute of Environmental and Occupational Health Sciences

College of Public Health

National Taiwan University

Master Thesis

使用受體模式結合手動採樣有機化合物與連續監測資料

探討臺北市細懸浮微粒污染源

Integrate Manual Sampling Data of Organic Markers and

Continuous Monitoring Data to Perform Source

Apportionment in Taipei

劉弈紘

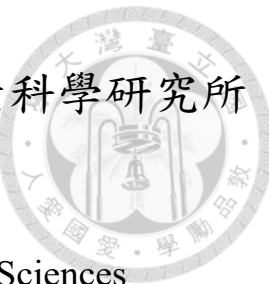
Yi-Hsien Liu

指導教授：吳章甫 博士

Adviser: Chang-Fu Wu, Ph.D.

中華民國 112 年 7 月

July 2023





序言

在完成本研究期間，我要向許多人致以最誠摯的感謝。加入吳章甫老師實驗室的期間，接受到老師及前輩們給予寶貴的建議和指導，使我能夠完成這項研究。兩年前的我一定難以想像在碩士生涯中能夠學習的量，挖掘自己的潛力看見了更多可能，未來一定還能更加成長，而這一切都多虧了每一個幫助我的人。

首先是我的指導教授吳章甫教授，老師讓我在碩士生涯中深刻體會到從學生跨入能獨當一面的專業應該具備甚麼樣的能力。在給予適當信任下提點我該注意甚麼才能讓思考更加完善，對於學習來說十分有幫助。而實驗室的各位前輩，特別感謝 Aris 學長和 Mike 學長，在我遇到問題時從不吝嗇給予我知識及資源，因為有你們讓我的學習更加順利且如有後盾般安心。另外還有冠霖和曼妮，也非常感謝冠霖後來接手了採樣的工作，讓我能持續專心在研究和分析上。感謝曼妮在日常中還有最需要穩定心情時，用你的自信開朗感染我、當我的心靈支柱。

UPLC-MS/MS 研究方法的部分，非常感謝陳家揚老師實驗室的協助。則穎學長除了幫助技術上方法的建立之外，還很有耐心的說明各式各樣的問題。還有宜健在我上機遇到狀況最恐慌之時，給予及時的回應及幫助。

再來是感謝研究所的各位朋友們，不管是從大學以來還是這兩年才認識的各位，我永遠不會忘記這兩年內超密集又很溫馨的慶生活動。在繁忙、壓力很大的時候，大家齊聚一堂聊天吃東西是最好的療癒。

最後要感謝我的家人和靖丰，對於我做的每個決定都給予最大程度的尊重，還有最重要的支持與陪伴。

再次感謝所有幫助過我的人，你們的支持對我來說意義非凡。



中文摘要

細懸浮微粒 (PM_{2.5}) 對人體及生態的危害眾所皆知，因此掌握 PM_{2.5} 的來源及貢獻量對空氣品質政策的制定十分重要。透過正矩陣因子分解受體模式 (PMF) 從受體點量測到的濃度資料追溯其來源和貢獻量，可以提供空氣品質政策科學上的建議。

PM_{2.5} 成分在線式監測儀器可以隨時監測元素、離子等化學物質以獲得成分小時值，而在過去 PMF 相關的研究中這些高時間解析度的資料能有效的解析污染源。也有研究表示加入有機化合物更可增強污染源的識別，特別是二次有機氣膠對於追蹤污染源有重要的價值。這些研究強調了有機化合物在 PMF 中的重要性，但大多受到採樣方法的限制使時間解析度較低。同時納入在線式監測高時間解析度以及有機化合物低時間解析度的研究較少，因此本研究嘗試結合兩者進行分析。

本研究於 2022 年 11 月至 2023 年 4 月，在台灣台北市大安空氣品質測站進行採樣。手動採樣使用石英濾紙，每次採樣 12 小時，並使用極致液相層析串聯質譜儀 (UPLC-MS/MS) 分析選定的有機化合物。結合測站連續監測的小時成分資料，使用多重線性引擎 (ME-2) 進行多重時間解析度的源解析。

使用 PMF 分析時分成模型一及模型二。模型一包含了 24 種成分測站的物種，模型二則額外增加 7 種作為特定污染源指標的有機化合物。模型一解析出六種污染源，分別是：交通 (22.4%)，揚塵 (4.5%)，燃油燃燒 (17.4%)，煤炭燃燒/工業 (27.3%)，工業 (6.5%) 和海鹽 (13.1%)。模型二相較於模型一還額外辨識出名為「生物源」的污染源，特徵物種包含 2-methylerythritol (2-MT) 和 arabinol。透過逆軌跡模式得到這些生物性氣膠可能來自台北市周邊山區或是宜蘭。另外，還透過 levoglucosan 和 succinic acid 辨識了可能潛在混合於交通源中的生質燃燒污染。

本研究凸顯了 PMF 分析在包含有機成分後能改善預測結果，多辨識出了一種污染源是與過去研究不同之處。此結果也讓未來在考量針對台北市的污染源進行管控時，提供一定的科學依據。




關鍵詞：正矩陣因子解析，細懸浮微粒，有機氣膠，極致液相層析串聯質譜儀，多重時間解析度

Abstract

Air pollution, particularly fine particulate matter (PM_{2.5}), has significant adverse health effects and contributes to atmospheric visibility reduction and global climate change. Understanding the distribution and sources of PM_{2.5} is crucial for effective air quality management. Receptor models, such as Positive Matrix Factorization (PMF), can help identify pollution sources by analyzing ambient concentration data at receptor sites.

Online monitoring instruments for PM_{2.5} composition allow real-time measurement of elements, ions, organic carbon (OC), and elemental carbon (EC), enabling the detection in hourly patterns. PMF modeling, combined with these measurements, effectively explores PM_{2.5} contributions. Adding organic compounds enhances the identification of pollution sources, particularly secondary organic aerosols (SOA) in tracking pollution sources. Previous studies emphasized the importance of organic tracers in PMF modeling, but most have faced limitations in time resolution due to manual field sampling. Few investigations have incorporated both low time resolution data of organic compounds and high time resolution data from online monitoring.

This study was conducted from November 2022 to April 2023 at the Daan Air Quality Monitoring Station in Taipei, Taiwan. Manual sampling was performed using

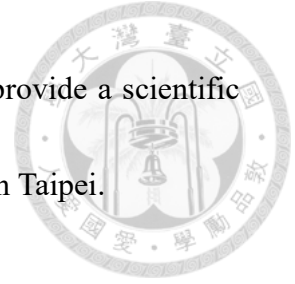


quartz filters, with each sampling period lasting 12 hours. The selected organic compounds were analyzed using ultra-performance liquid chromatography-tandem mass spectrometry (UPLC-MS/MS). To integrate the hourly component data obtained from the continuous monitoring at the station, a multilinear engine (ME-2) was employed for source apportionment.

The study aimed to identify and apportion pollution sources using the PMF model. Two models were implemented in this study: Model 1, which included 24 species, and Model 2, which included an additional 7 organic species. For Model 1, it was found that the optimal solution consisted of 6 factors: traffic (22.4%), dust (4.5%), oil combustion (17.4%), coal combustion/industry (27.3%), industry (6.5%), and sea salt (13.1%). In Model 2, an additional source called "Biogenic Source" was identified. This source was characterized by the presence of 2-methylerythritol (2-MT) and arabitol, which are indicators of biogenic aerosols. The backward trajectory analysis indicated that these aerosols originated from surrounding mountainous areas and peripheral regions. Furthermore, the potential biomass burning pollution in the identified traffic-related pollution source was identified through the presence of levoglucosan and succinic acid.

The study highlighted the improved performance of the PMF model with the inclusion of organic components, as it allowed the identification of the biogenic source,

which was not previously observed in field studies. The findings provide a scientific basis for future considerations and regulations regarding pollution in Taipei.



Keywords: Positive Matrix Factorization, Fine Particulate Matter; Organic marker,

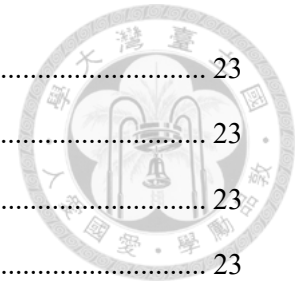
UPLC-MS/MS, Multiple time resolution



Contents

序言.....	i
中文摘要.....	ii
Abstract.....	iv
Contents.....	vii
List of Figures.....	ix
List of Tables.....	x
List of Appendixes.....	xi
Chapter 1 Introduction.....	1
1.1. Background.....	1
1.2. Receptor model.....	2
1.3. Importance of organic tracers in PMF.....	3
1.4. Study aims.....	7
Chapter 2 Materials and methods.....	9
2.1. Sampling site.....	9
2.2. Study Period.....	11
2.3. Sampling instruments.....	11
2.4. Chemical analysis of organic tracers.....	12
2.4.1. Organic compounds analysis.....	12
2.4.2. Data Quality.....	15
2.5. Receptor model (PMF).....	15
2.6. Data preprocessing.....	17
2.6.1. Calculations of uncertainties.....	17
2.6.2. Model parameter settings.....	19
2.6.3. Source profile interpretation.....	20
2.6.4. Mass Reconstruction.....	21
2.7. PMF modeling.....	22

Chapter 3 Results and Discussions.....	23
3.1. Summary statistics and data pretreatment	23
3.1.1. Mass reconstruction.....	23
3.1.2. Data pretreatment	23
3.2. Factor Identification	26
3.2.1. Factor Identification of Model 1.....	26
3.2.2. Factor Identification of Model 2.....	35
3.2.3. Seasonal variation.....	47
3.3. Sensitivity analysis	51
3.4. Limitations.....	52
Chapter 4 Conclusions and recommendations.....	54
References	56
Appendixes.....	66



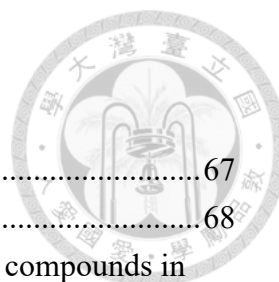


List of Figures

Figure 1 Scheme of this study for source identification	8
Figure 2 Sampling site map	10
Figure 3 The calculation of major chemical component of mass reconstruction (non-sea-salt SO_4^{2-} : $\text{SO}_4^{2-} - 0.252[\text{Na}^+]$) (Chow et al., 2015)	22
Figure 4 IM/IS of Model 1 and Model 2.....	27
Figure 5 The schematic diagram of Model 1 and Model 2.....	27
Figure 6 Source profiles of each chemical species of Model 1 (black bars denote concentration; gray points denote explained variation)	28
Figure 7 Diurnal plot of Model 2.....	29
Figure 8 The contribution of six sources and the reconstructed trend of $\text{PM}_{2.5}$ concentration (RPM) of Model 1	33
Figure 9 Estimation of the source of coal combustion/industry by backward trajectory HYSPLIT model (24-hour duration)	34
Figure 10 Source profiles of each chemical species of Model 2 (black bars denote concentration; gray points denote explained variation)	37
Figure 11 The contribution of six sources and the reconstructed trend of $\text{PM}_{2.5}$ concentration (RPM) of Model 2.....	39
Figure 12 Estimation of the source of biogenic source by backward trajectory HYSPLIT model (24-hour duration)	40
Figure 13 Correlation between levoglucosan and K (after excluded the outliers $R^2= 0.15$).....	43
Figure 14 Correlation between biomass burning markers (levoglucosan and succinic acid) and traffic markers (Cu and Ba)	43
Figure 15 Concentration of cholesterol.....	45
Figure 16 Factor contribution of three seasons.....	47
Figure 17 Estimation of the source of oil combustion source by backward trajectory HYSPLIT model (24-hour duration)	48
Figure 18 Proportion of the source contribution.....	52

List of Tables

Table 1 Summary of the organic markers of target sources.....	6
Table 2 Gradient separation of Method 1 and Method 2	14
Table 3 The summary of data pretreatment	19
Table 4 Summary statistics of PM _{2.5} components data collected at Daan AQS (ng/m ³)	25
Table 5 The sources corresponding to the organic compounds in this study	38
Table 5 Atmosphere concentrations of cholesterol of previous studies	46
Table 6 Summary of contributions of biogenic source in previous study....	49
Table 7 The average concentration of traffic-related pollutants in this study and those measured by nearby ground-level monitor (ppm)	50



List of Appendixes

Appendix 1 Calibration curves of 8 organic compounds.....	67
Appendix 2 Sampling dates marked as color blue.....	68
Appendix 3 IS, Matrix spike recovery rate, and MDL of 8 compounds in UPLC-MS/MS analysis	69
Appendix 4 Mass reconstruction exceeding $\pm 40\%$ of measured PM _{2.5} of each month.....	70
Appendix 5 Decisions for double counting deletion.....	71
Appendix 6 The presentation of peaks of 8 compounds in UPLC-MSMS analysis.....	72
Appendix 7 Summary of organic compounds concentrations in other studies	73



Chapter 1 Introduction

1.1. Background

Exposure to air pollutants such as fine particulate matter (PM_{2.5}) causes both acute and chronic adverse health effects (Jiménez et al., 2009; Mimura et al., 2014), and it could lead to negative effects on atmospheric visibility and global climate change (Keim et al., 2005; Long et al., 2023). According to WHO, air pollution was responsible for 4.2 million deaths in 2016, and it was estimated to cause about 29% of lung cancer deaths, 43% of COPD deaths, 25% of ischaemic heart disease deaths, and 24% of stroke deaths.

(<https://www.who.int/data/gho/data/themes/topics/indicator-groups/indicator-group-details/GHO/ambient-air-pollution>)

PM_{2.5} is a mixture of pollutants and can be contributed by various types of air pollution sources. Recently, more and more studies focus on source-specific PM_{2.5} and associated composition because the PM_{2.5} constituent varies with sources and they may specifically affect human health (Achilleos et al., 2017; Chen & Lippmann, 2009; Kelly & Fussell, 2012; Stanek et al., 2011; Yan et al., 2022). For example, biomass burning was found to be associated with CVD mortality (Achilleos et al., 2017) while the magnitude of estimated risks from the sea salt were smaller (Mar et al., 2006). Many




studies have evaluated the concentration, chemical composition, and sources of $PM_{2.5}$ to obtain a better understanding of air pollution.

1.2.Receptor model

The receptor model can clarify the relationship between sources and the receptor, which helps to identify where air pollution might come from by measuring ambient concentration at a receptor site (Watson, 1984). Source apportionment studies employ receptor models, such as Positive Matrix Factorization (PMF), to conduct source-specific analyses. PMF is widely used in such studies due to its effectiveness. Compared to other models, such as chemical mass balance (CMB) model, PMF requires less prior knowledge of emission profiles and incorporates a weighting scheme that considers the uncertainties associated with measured concentrations. By adjusting the uncertainty estimates, PMF can handle below-detection-limit values and missing data more effectively (Almeida et al., 2020).

In the application of the PMF model for identifying sources of observed $PM_{2.5}$ chemical species, various measurements are typically used as input data, including inorganic ions, elements, organic carbon (OC), and elemental carbon (EC). Organic compounds could be also used as marker species to identify major sources of the observed $PM_{2.5}$ (Heo et al., 2013; Schauer et al., 1996; Simoneit, 1985). Organic compounds can be divided into two types. Primary organic aerosols (POA) refer to




those directly emitted into the atmosphere, while secondary organic aerosols (SOA) are formed through oxidation, condensation, and multiphase chemical processes involving gaseous precursors (Pandis et al., 1992). By analyzing the composition and characteristics of these species, the PMF model can help identify the different sources contributing to PM_{2.5} pollution.

1.3.Importance of organic tracers in PMF

Nowadays, online monitoring instruments for PM_{2.5} composition have been developed. These instruments measure elements, ions, OC/EC in high time resolution (Bauer et al., 2009; Liu et al., 2019; Young et al., 2016), thus effectively capturing the concentration changes in different species over time and enabling the detection of daily source patterns. PMF has been implemented with online monitoring measurements to explore the PM_{2.5} contributions (Gao et al., 2016; Ho et al., 2018). On the other hand, analyzing organic compounds usually takes large resources with off-line techniques to obtain the data compared to inorganic and elemental analyses. Therefore, it is necessary to assess the additional performance enhancement of adding organic compounds in PMF modeling.

A 24-h integrated PM_{2.5} sampling program was conducted to characterize PM_{2.5} in the capital of South Korea, Seoul, which is one of the mega-cities in Northeast Asia. It could be affected by a variety of sources of emissions and transport from outside, which




is similar to Taipei. This study examined the effectiveness of adding organic compounds as input data in the PMF model. Adding organic compounds separated the characteristics of biogenic sources from the source profiles that were obtained based on inorganic species only. By doing so, the correlations between the observed PM_{2.5} and the predicted PM_{2.5} were also improved (Shin et al., 2022).

Another study in Hong Kong showed the importance of SOA tracers (Hu et al., 2010). In PMF analysis, the primary and secondary source contributions to OC in PM_{2.5} were determined by considering major inorganic compounds and organic tracers. This study emphasized that SOA tracers gave a specific identification in PMF profile, such as phthalic acid could trace back to Naphthalene, which was from vehicular emission. This signifies that the inclusion of SOA tracers plays a crucial role in identifying SOA components. One advantage of utilizing these SOA tracers is their specificity for a wide range of SOA precursor classes. Therefore, the inclusion of SOA tracers provides valuable insights into the characterization and identification of SOA sources in PM_{2.5}.


These studies highlight the importance of organic tracers in PMF modeling, but the time resolution was low due to the limitation of manual field sampling. Relatively few studies have been performed incorporating low time resolution data of organic compounds and high time resolution of online monitoring data.

In this study, three SOA tracers and five POA tracers were selected (Table 1) for



identifying their corresponding sources. 2-methylerythritol (2-MT) is the secondary tracer for isoprene, which was emitted from the biogenic source (Ion et al., 2005). 2,3-dihydroxy-4-oxopentanoic acid (DHOPA) is the secondary tracer for toluene, which was the emission of solvent use (Hopke, 2016; Kleindienst et al., 2004; Kleindienst et al., 2007). Phthalic acid is the secondary tracer for Naphthalene, which is the emission of vehicles and incomplete combustion of carbonaceous materials (Wang et al., 2015). As for POA, levoglucosan, succinic acid, cholesterol, arabitol, and mannitol were selected. Levoglucosan is produced by the thermal alteration of Carbohydrates and starch which is a marker for biomass burning (Bhattarai et al., 2019; Chan et al., 2005). Arabitol and mannitol are key components of fungal spores (Bauer et al., 2008). Succinic acid is one of the low molecular weight dicarboxylic acids (DCAs), which accounts for an appreciable fraction of the WSOC in biomass-burning aerosols (Akhtar et al., 2014; Falkovich et al., 2005). Cholesterol is emitted from food cooking (Rogge et al., 1991).

Table 1 Summary of the organic markers of target sources



Compounds	Type	Sources	References
2-MT	Secondary (Isoprene)	Biogenic	(Edney et al., 2005; Ion et al., 2005)
DHOPA	Secondary (Toluene)	(1) Solvent use (2) Traffic related (3) Biomass burning	(Ding et al., 2017; Kleindienst et al., 2004; Kleindienst et al., 2007)
Levogluconan	Primary	Biomass burning	(Bhattarai et al., 2019; Chen & Lippmann, 2009)
Phthalic acid	Secondary (Naphthalene)	(1) Vehicular emission (2) Aromatic compounds	(Wang et al., 2015)
Arabitol	Primary	Fungal spores	(Bauer et al., 2008; Golly et al., 2019)
Mannitol	Primary		
Succinic acid	Primary	(1) Photo-oxidation of unsaturated fatty acid (from Plants and Domestic cooking) (2) Biomass burning	(Akhtar et al., 2014; Dai et al., 2011)
Cholesterol	Primary	Cooking marker	(He et al., 2004; Rogge et al., 1991)

1.4. Study aims

The main purposes of this study are to:

- (1) Combine high time resolution online monitoring data and low time resolution organic compounds data in PMF modeling.
- (2) Examine the effectiveness of the organic tracers brought to the factor identification in PMF.

The overall study design is shown in Figure 1.



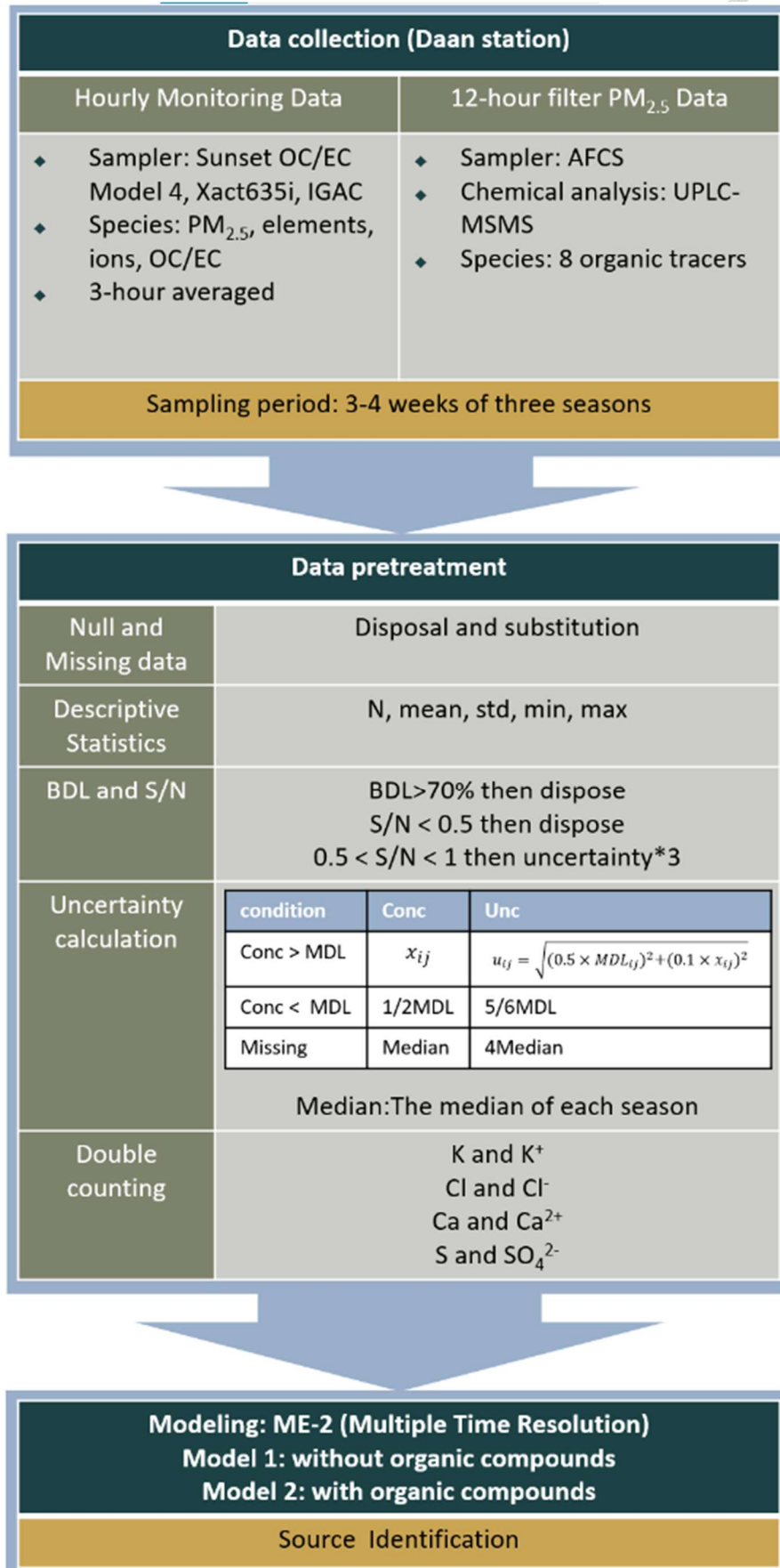


Figure 1 Scheme of this study for source identification

Chapter 2 Materials and methods



2.1. Sampling site

Taipei, the capital city in Taiwan with a population exceeding 2.6 million, faces a notable vulnerability to air pollution. This susceptibility is attributed to its geographical location within a basin, encircled by mountains, and characterized by a high population density. Though the concentration of PM_{2.5} in Taipei was decreasing year by year due to the implementation of air pollution controlling plan, the annual concentration of $14.01 \pm 1.94 \mu\text{g}/\text{m}^3$ (臺北市政府環境保護局, 2021) was still above the recommended concentration of WHO Global air quality guidelines ($10 \mu\text{g}/\text{m}^3$). The online PM_{2.5} composition measurements used in this study were collected at the Daan air monitoring station (Figure 2), which is located at the bustling and densely populated area in Taipei. The station is 4 floors above the ground, situated on Zhongxiao East Road, which is a major thoroughfare that connects several important neighborhoods in the city. The measured data including temperature, wind speed, humidity, and air pollutant concentrations such as PM_{2.5}, PM₁₀, ozone (O₃), nitrogen dioxide (NO₂), sulfur dioxide (SO₂), elements, OC/EC, etc.

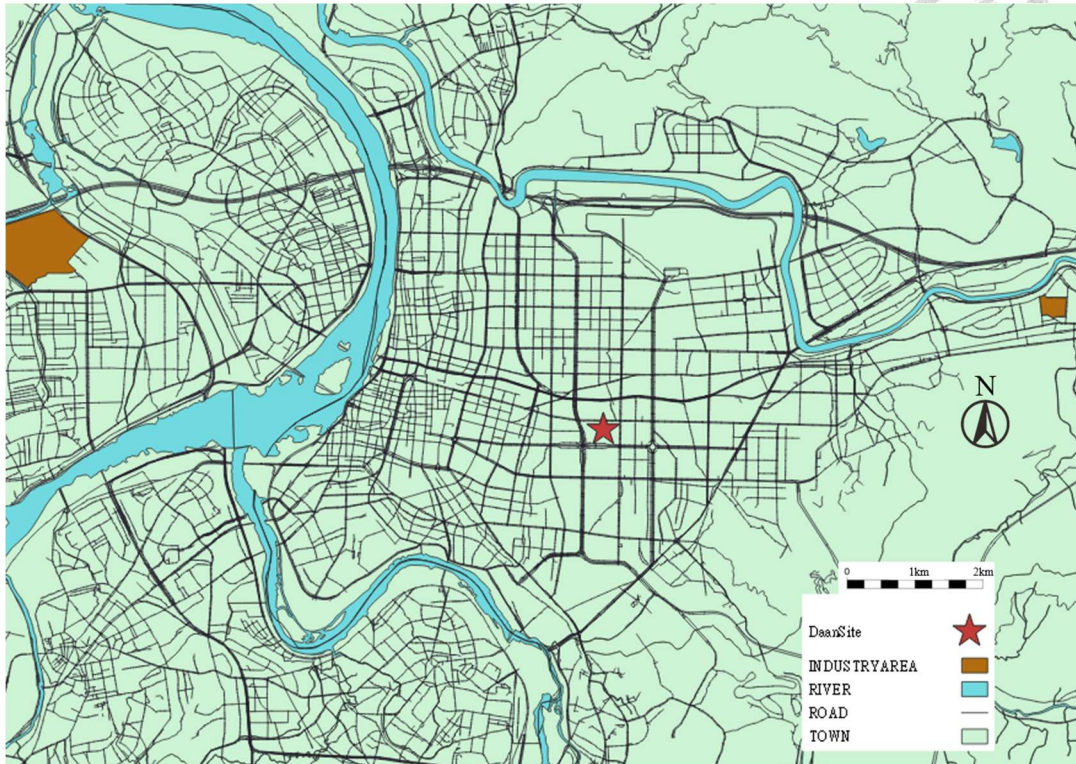


Figure 2 Sampling site map



2.2. Study Period

The study was designed to collect data of three seasons. Transported pollutants brought by northeast monsoons from neighboring countries could cause a significant impact on the air quality in northern Taiwan during winter. Therefore, the field sampling was conducted for three to four weeks in each season (Appendix 2) so that the results could be compared between seasons. The data of Daan monitoring station from November, 2022 to April, 2023 was used in this study.

2.3. Sampling instruments

Two Automatic Filter-Changing Samplers (AFCS, PNS 16T-6.3, Comde Derenda; Germany) were used to collect 12-hour filter samples, which was also applied in previous studies (Siudek & Ruczyńska, 2021; Yarkin et al., 2020). Two filters were collected at the same time for 12 hours. AFCS automatically transferred the new filter to the sampling position, and when the sampling was done, the sampled filter would be transferred back to the cooling chamber. Samples were collected at the flow rate of 38.4 L/min, and the flow rate were checked before and after sampling. The Whatman® QM-A quartz filters (2.2 μm , 47 mm) were used, and filters were pre-baked at 900 °C for 4 hours to prevent the residual organic compounds on filters before sampling. Each sampled filter was preserved in the petri dish, wrapped with parafilm, and stored at -4 °

C until chemical analysis.

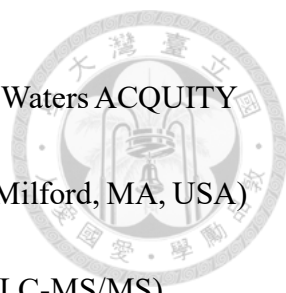
Sunset OC/EC Model 4 was used to measure the OC/EC concentration. The Xact625i (Cooper Environment Services, OR, USA) using energy dispersive X-ray fluorescence (ED-XRF) method was operated to measure forty-two PM_{2.5} elemental compositions. Eleven water-soluble ions were analyzed using an In-situ Gas and Aerosol Composition monitor (IGAC Model S-611EG, Machine Shop, Fortelice International Co., Ltd., Taiwan) with an ion chromatography (IC) system.



2.4. Chemical analysis of organic tracers

2.4.1. Organic compounds analysis

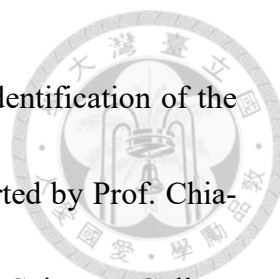
To identify the possible organic aerosol sources more specifically, this study collected 12-hour time-integrated filter samples for chemical analysis of PM_{2.5} organic components. Two filters from the same period of time were analyzed as one sample because the doubled mass could be helpful in the UPLC-MS/MS analysis. Isotopes of selected organic markers were used as internal standards (IS) for quality control. Each sample was spiked with 1 µg IS, followed by vortex mixing for 30 seconds, ultrasonic extraction using 10 mL of methanol for 20 min, and separation to obtain the supernatant. The resulting extracts were filtered through a 0.22 µm polytetrafluoroethylene (PTFE) filter, and the filtered extract was preserved in the amber vial for the following



chromatography analysis. 5 μ L of the final extract was injected into a Waters ACQUITY Ultra Performance Liquid Chromatography I-Class system (Waters, Milford, MA, USA) coupled with a Waters Xevo TQ-XS tandem mass spectrometer (UPLC-MS/MS).

Two protocols were used for analyzing the organic compounds. Method 1 was designed for the analysis of 2-MT, DHOPA, levoglucosan, phthalic acid, succinic acid, arabitol, and mannitol using a Hypercarb column (2.1 mm x 50 mm, 3 μ m). Method 2 was designed for the analysis of cholesterol using a CSH Phenyl-Hexyl column (3.0 mm x 50 mm, 1.7 μ m). Method 1 was operated with UniSpray in negative mode, whereas APCI positive mode was used in Method 2. Ions were monitored with multiple reaction monitoring (MRM) modes. The gradient separation of Method 1 was conducted with 0.05% NH_4OH (v/v) in water (eluent A) and acetone (eluent B), and Method 2 was conducted with deionized water (eluent A) and methanol (eluent B). Details of the gradient separation are listed in Table 2. Please refer to Chou (2021) and Albinet et al. (2019) for detailed information on organic component analysis.

To identify the compounds, the retention times of the LC peaks and the ion spectra were compared with those of certified standards. Calibration standards were prepared by adding different quantities of certified standards and a known amount of IS on quartz filters. Calibration curves were then constructed by plotting the peak area ratios between the calibration standards and IS against the concentrations of the calibration



standards. This approach allowed for accurate quantification and identification of the compounds in the samples. These methods were technically supported by Prof. Chia-Yang Chen from Institute of Environmental and Occupational Health Sciences, College of Public Health, National Taiwan University.

Table 2 Gradient separation of Method 1 and Method 2

	Method 1			Method 2		
Column	Hypercarb			CSH Phenyl-Hexyl		
Oven temperature (°C)	35			40		
Flow rate (mL/min)	0.2			1.0		
Injection volume (µL)	5			5		
Mobile phase	A: 0.05% NH ₄ OH (aq) B: Acetone			A: Water B: Methanol		
Gradient	(min)	A (%)	B (%)	(min)	A (%)	B (%)
	0	97	3	0	70	30
	1.5	97	3	0.5	70	30
	3	0	100	3	0	100
	4.5	0	100	4	0	100
	5.5	97	3	4.2	70	30
	8	97	3	6.5	70	30



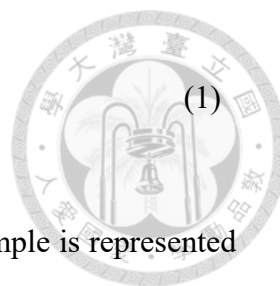
2.4.2. Data Quality

Lab and field blank samples were also collected and measured for QA/QC and/or blank subtraction. The limits of detection (LOD) and quantification (LOQ) were determined as the lowest analyte concentration that yields a signal-to-noise ratio of 3 and 10, respectively. Method Detection Limit (MDL) were determined as three times standard deviation of 7 blank filters. Details of the compound spike recovery and MDL are listed in Appendix 3.

The matrix effect was tested by the post-extraction spiked method before the analysis of real samples. Matrix-containing recoveries of spiked samples fell within 80 to 120% (Appendix 3), which meant that potential interference could be ignored. Each batch of samples (14 samples) was conducted with two field blanks and one lab blank. For each batch of samples, one calibration curve was conducted ($R^2 > 0.990$), and the concentration of samples should fall within the range of the calibration curve.

2.5. Receptor model (PMF)

The application of PMF involved using a bilinear receptor model based on the concept of a mass balance equation. This approach was employed to identify and quantify potential sources of the observed air pollution levels (Paatero and Tapper, 1994). The model is written as:



$$x_{ij} = \sum_{k=1}^p g_{ik}f_{kj} + e_{ij} \quad (1)$$

The measured concentration of the j^{th} chemical species in the i^{th} sample is represented by x_{ij} . The contribution from the k^{th} source factor to the i^{th} sample is denoted as g_{ik} . The source factor, f_{kj} , is associated with a real-world source profile, which defines the fraction of the j^{th} chemical species in the k^{th} source. The residual term is represented by e_{ij} , and p represents the number of sources

The factor contributions and profiles are derived by minimizing the objective function Q :

$$Q = \sum_{i=1}^n \sum_{j=1}^m \left[\frac{x_{ij} - \sum_{k=1}^p g_{ik}f_{kj}}{u_{ij}} \right] \quad (2)$$

where u_{ij} is the uncertainty that corresponds to the j^{th} species in the i^{th} sample, n is the number of samples, and m is the number of species, representing the size of the measured concentration matrix.

In this study, The Multilinear Engine (currently in its second version, ME-2) was applied for PMF modeling of the multiple time resolution data. ME-2 is a flexible PMF variation applicable to chemically-speciated pollutants considering the different time scales (Crespi et al., 2016; Kuo et al., 2014; Liao et al., 2015; Liao et al., 2013; Ogulei et al., 2005). To integrate the data in PMF model, the original bilinear CMB equation of PMF is adjusted as (Zhou et al., 2004):

$$x_{sj} = \frac{1}{t_{s2} - t_{s1} + 1} \sum_{k=1}^P \left[\left(\sum_{i=t_{s1}}^{t_{s2}} g_{ik} \right) f_{kj} \right] + e_{sj} \quad (3)$$



where x_{sj} is the measured concentration of species j in sample s . t_{s2} is the end of time, while t_{s1} is the start of the time for sample s . The time unit is “hour” which is consistent with the high time resolution data. F_{kj} denotes the concentration of species j in source profile p , and g_{ik} denotes the normalized time series of source p . P denotes the total number of sources and e_{sj} is the residual term.

The fraction $\frac{1}{t_{s2}-t_{s1}+1}$ in the formula means taking the average over the sampling time for individual sample x_{sj} . For the low time resolution organic compounds data, $t_{s2} = 12$ (hour), $t_{s1} = 1$ (hour), so the contribution is divided by 12 hours. To highlight the organic compounds in the model, the hourly data were averaged into 3-hour data and thus $t_{s2} = 3$, $t_{s1} = 1$ (hour). The ratio of high resolution and low resolution changed from $1:\frac{1}{12}$ to $1:\frac{1}{4}$, which meant that the importance of organic compounds increased in this model. The fitting performance of the MTR model is verified by previous researches (Sofowote et al., 2021).

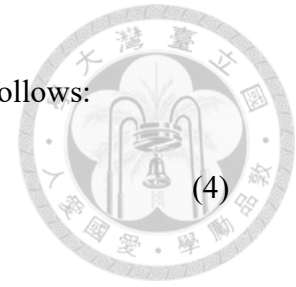
2.6. Data preprocessing

2.6.1. Calculations of uncertainties

The associated uncertainties (u_{ij}) of measurements were calculated from method

detection limit (MDL) and mass concentration. The equation is as follows:

$$u_{ij} = \sqrt{(0.5 \times MDL_{ij})^2 + (0.1 \times x_{ij})^2} \quad (4)$$



where MDL_{ij} is the MDL of the j^{th} species in the i^{th} sample. If the measured mass concentration fell below MDL, it was replaced with half of the MDL value, and the corresponding uncertainty was set as 5/6 of the MDL value. In cases where values were missing, they were replaced by the median value of the season and their uncertainties were set as four times the median (G. Norris et al., 2014). The summary of the data pretreatment are shown in Table 3.



Table 3 The summary of data pretreatment

Condition	Concentration	Uncertainty
Conc > MDL	x_{ij}	$u_{ij} = \sqrt{(0.5 \times MDL_{ij})^2 + (0.1 \times x_{ij})^2}$
Conc < MDL	1/2MDL	5/6MDL
Missing	Median	4Median

2.6.2. Model parameter settings

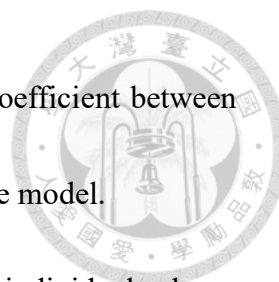
Signal-to-noise ratio (S/N) is a parameter for qualities of species:

$$\text{if } x_{ij} > s_{ij}, \text{ then } d_{ij} = (x_{ij} - s_{ij})/s_{ij}$$

$$\text{else if } x_{ij} < s_{ij}, \text{ then } d_{ij} = 0$$

$$\left(\frac{S}{N}\right)_j = \frac{1}{n} \sum_{i=1}^n d_{ij} \quad (5)$$

where x_{ij} represents the mass concentration of the j^{th} species in the i^{th} sample, and s_{ij} represents the corresponding uncertainty. S/N greater than 1 indicates a species with a “good” signal. The species with S/N greater than 0.5 but less than one were categorized as “weak”, and S/N less than 0.5 were categorized as “bad” in quality. The uncertainties of “weak” variables were down-weighted by tripling their original uncertainties. The variables categorized as “bad” and those with more than 70% missing and below method detection limit (BDL) values were excluded from the model (Kuo et al., 2014;



Paatero & Hopke, 2003). The species with Spearman correlation coefficient between observed and predicted values smaller than 0.6 was omitted from the model.

The maximum individual column mean (IM) and the maximum individual column standard deviation (IS) were used to determine the appropriate number of sources. The equations of these two indicators are as below:

$$IM = \max_{j=1\dots m} \left(\frac{1}{n} \sum_{i=1}^n r_{ij} \right) \quad (6)$$

and

$$IS = \max_{j=1\dots m} \left(\sqrt{\frac{1}{n-1} \sum_{i=1}^n (r_{ij} - \bar{r}_i)^2} \right). \quad (7)$$

where r_{ij} is the scaled residual of the j^{th} species in the i^{th} sample, and r_{ij} is calculated as residual divided by uncertainty. These two indicators represent the least fit of species in the factor solution. When the number of factors reaches a critical value, IM and IS will experience a significant drop (Lee et al., 1999).

2.6.3. Source profile interpretation

The source profile was interpreted by the explained variation (EV) of each species, which was used to compare the importance of each species in the source (Anttila et al., 1995; Lee et al., 1999). EV is calculated as:



$$EV_j = 1 - \frac{\sum_{i=1}^n \frac{e_{ij}^2}{\sigma_{ij}^2}}{\sum_{i=1}^n \frac{x_{ij}^2}{\sigma_{ij}^2}} \quad (7)$$

where e_{ij} is the residual for the j^{th} species in the i^{th} sample. EV_j should be less than or equal to 1

2.6.4. Mass Reconstruction

The purpose of mass reconstruction is to identify potential measurement errors and assess data quality by comparing the calculated sum of the main components within $PM_{2.5}$ with the measured mass concentration of $PM_{2.5}$.

The $PM_{2.5}$ mass reconstruction is primarily calculated using seven chemically representative components (Figure 3), with the following formula (Chow et al., 2015) :

$$RPM_{2.5} = [OM] + [EC] + [SIA] + [CM] + [SS] + [TE] + \text{others} \quad (8)$$

The "others" component represents uncalculated or unidentifiable constituents. It should be noted that the element Al (aluminum) was not measured at the Daan station. Therefore, the calculation for $PM_{2.5}$ mass reconstruction in this project does not include Al. However, since metals usually account for a small proportion within $PM_{2.5}$, its exclusion is not expected to significantly impact the calculation results.

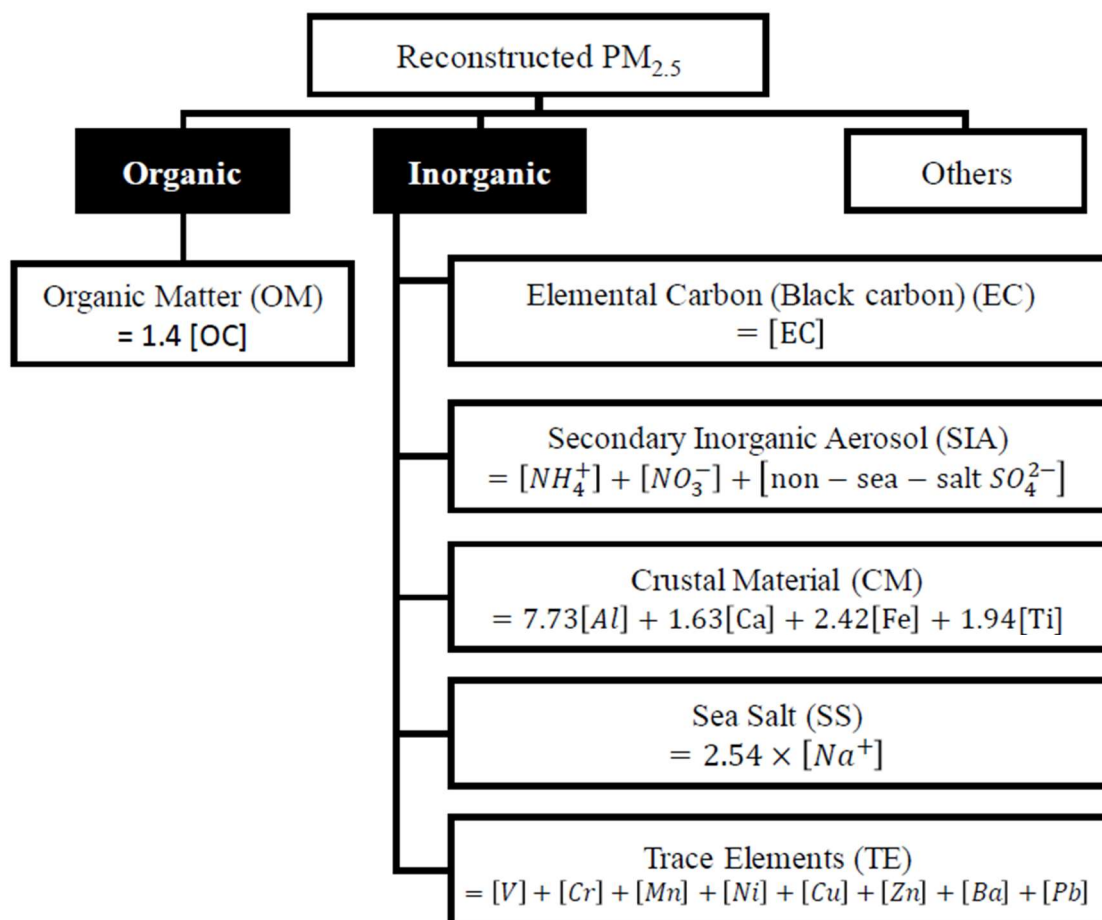


Figure 3 The calculation of major chemical component of mass reconstruction (non-sea-salt SO_4^{2-} : $SO_4^{2-} - 0.252[Na^+]$) (Chow et al., 2015)

2.7. PMF modeling

Two different time resolution of $PM_{2.5}$ compositions were collected in this study. The 12-hr filter samples were analyzed for 8 organic acid components. This study used the data of Daan monitoring station from November, 2022 to April, 2023. The hourly monitored measurements included 43 heavy metal elements, 2 carbon components, 10 water-soluble ions, and the 12-hour time integrated samples included 8 organic compounds. The main sources of $PM_{2.5}$ affecting the air quality in Taipei City were

estimated by PMF model with multiple time resolution data.



Chapter 3 Results and Discussions


3.1. Summary statistics and data pretreatment

3.1.1. Mass reconstruction

In the application of the Chemical Mass Balance model for source apportionment of pollution, the reasonable difference between the "observed PM_{2.5}" and the "mass reconstructed PM_{2.5}" is defined as 100% ± 20% (Watson, Chow et al. 2004). However, this range is mostly applied to daily data. Considering that the hourly data may contain higher variability, 40% difference was selected as the screening criterion in this study to examine the data quality of PM_{2.5}. Unfortunately, the data quality of November did not meet the standard. The values that were out of standard (100% ± 40%) accounted for 52% of the PM_{2.5} measurements in November. (Appendix 4). As a result, reconstructed PM_{2.5} mass was used as the total variable in the PMF modeling (Walton et al., 2021).

3.1.2. Data pretreatment

To avoid duplicating concentration calculations, the following species were selected for modeling based on their better data quality and importance of source identification (Appendix 5): SO₄²⁻ (excluding S), element K (excluding K⁺), element Ca (excluding Ca²⁺), and Cl⁻ (excluding elemental Cl). To maintain the rationality and



consistency of the analysis, the data preprocessing followed the PMF operating guidelines of US Environmental Protection Agency (Gary Norris et al., 2014). The species with more than 70% missing and below method detection limit (BDL) values were excluded from the model, and signal-to-noise ratio (S/N) less than 0.5 were also excluded. If the Spearman correlation between the predicted and observed values of a species in the model is less than 0.6, it indicates bad performance of the model's prediction, and the species should also be removed (Huang et al., 2022). The Spearman correlation for Ba was less than 0.6. However, it was an important non-exhaust traffic emission indicator. Thus, Ba was kept in the model, and the uncertainty was down-weighted by 3 times to reduce their influence on the analysis results. The signal-to-noise ratio (S/N) for cholesterol was less than 0.5, and the model performance became worse after including cholesterol. Cholesterol was excluded from the input data. After processing based on the above conditions, a total of 24 species were used for PMF model analysis. The detailed summary statistics of PM_{2.5} components data are shown in Table 5.

Table 4 Summary statistics of PM_{2.5} components data collected at Daan AQS (ng/m³)

	Species	N	MDL	BDL (%)	Mean	SD	Min	Max		
<u>hourly on-line measurements</u>	PM _{2.5}	1385	2000	27	10191.21	6333.86	1889.46	39430.62		
	K	1653	1170	3	122.67	245.46	ND	4427.38		
	Ca	1653	300	2	66.77	69.48	3.03	641.83		
	Ti	1653	160	3	8.7	11.51	ND	141.93		
	V	1653	120	46	0.78	1.06	ND	10.6		
	Cr	1653	140	47	0.68	1.17	ND	26.03		
	Mn	1653	170	25	5.66	7.36	ND	69.17		
	Fe	1653	140	2	142.14	119.52	5.52	1386.89		
	Ni	1653	100	29	0.77	0.94	ND	12.25		
	Cu	1653	79	3	5.75	11.75	ND	207.98		
	As	1653	1900	14	25.37	30.54	ND	472.97		
	Zn	1653	67	3	1.14	0.91	ND	6.25		
	Se	1653	81	77	0.26	0.44	ND	3.57		
	Br	1653	100	7	4.92	4.06	ND	26.47		
	Ba	1653	39	71	4.31	25.58	ND	507.13		
	Pb	1653	130	35	3.55	13.23	ND	348.23		
	OC	1572	400	10	2749.56	1480.91	713.9	10653.3		
	EC	1572	200	24	482.39	292.83	54.97	2758.4		
	<u>12-hr Filter samples</u>	<u>UPLC-MS/MS</u>	Na ⁺	1490	50	21	248.59	144.58	ND	1172
			NH ₄ ⁺	1504	55	17	1168.18	1103.92	23.18	7397.6
Cl ⁻			1504	36	18	389.17	295.25	ND	4925.6	
NO ₂ ⁻			1504	45	60	77.1	105.71	ND	2127.8	
NO ₃ ⁻			1504	45	18	1458.07	1823.55	ND	12687.8	
SO ₄ ²⁻			1504	38	17	1865.57	1379.83	ND	7637	
2-MT			140	0.56	58	0.61	0.81	ND	4.91	
Levogluconan			140	0.61	0	16.98	11.11	4.11	69.35	
DHOPA			140	0.21	3	1.80	1.95	ND	9.06	
Phthalic acid			140	2.15	1	13.66	12.46	2.10	62.08	
<u>IGAC S611-EG</u>	Arabitol	140	0.24	20	2.27	2.89	ND	19.82		
	Mannitol	140	0.31	10	8.88	12.85	ND	76.26		
	Succinic acid	140	0.31	0	36.11	17.02	10.60	85.43		
	Cholesterol	140	0.00	60	0.38	0.43	ND	1.95		



3.2. Factor Identification

After data preprocessing, 3-hour averaged data of 24 species from Daan monitoring station were used for PMF model analysis, referred to as "Model 1". To evaluate the impact of organic components on the model results, an additional 7 organic species were included for PMF analysis, referred to as "Model 2". The hourly data was tested also, and the factor identification was similar to the results of 3-hour averaged data.

3.2.1. Factor Identification of Model 1

In order to determine the appropriate number of factors for pollution source apportionment, Model 1 was executed with 3 to 8 factors. Based on mathematical indicators IM (maximum individual column mean) and IS (maximum individual column standard deviation), it was inferred that the most likely range for the number of factors was between 5 and 6 (Figure 4). One of the factors in 5-factor solution were “sea salt” mixed with “traffic related”. The profiles of 6-factor solution were divided into different sources. Therefore, 6 factors were chosen as the optimal solution for Model 1. On the other hand, for Model 2, the most likely number of factors was 7 or 8. The “industry” was divided into two in the 8-factor solution. Thus, 7 factors were selected as the best solution for Model 2 (Figure 5).

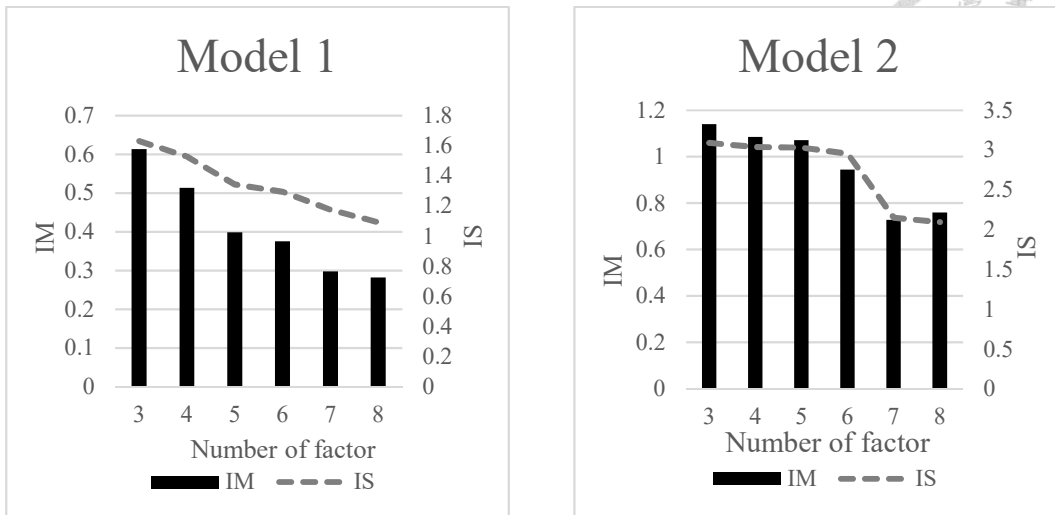


Figure 4 IM/IS of Model 1 and Model 2

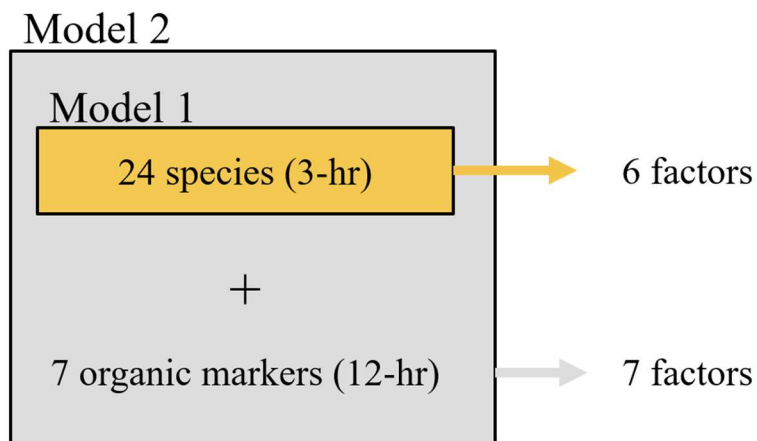


Figure 5 The schematic diagram of Model 1 and Model 2

The profiles of the 6 factors obtained from the PMF analysis of Model 1 are shown in the Figure 6. The factors were identified and named based on the indicator species within the profile ($EV > 0.4$).

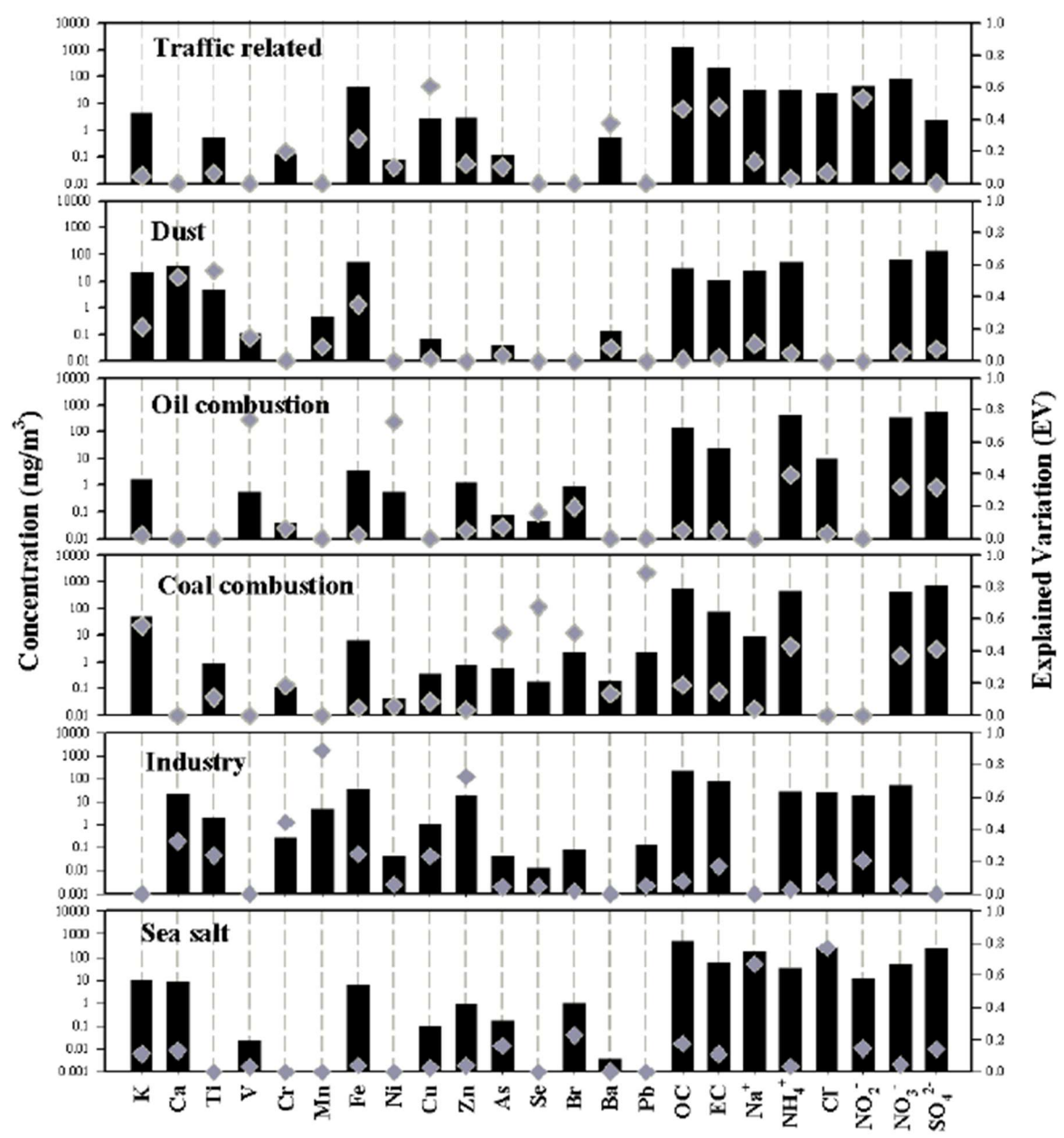
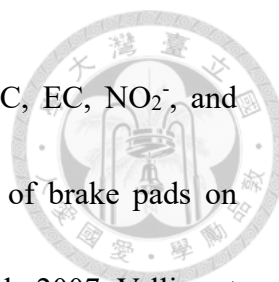


Figure 6 Source profiles of each chemical species of Model 1 (black bars denote concentration; gray points denote explained variation)



Traffic related source was identified by high EV of Cu, OC, EC, NO₂⁻, and moderate EV of Ba. Cu potentially originated from the abrasion of brake pads on vehicles during their operation (Gugamsetty et al., 2012; Querol et al., 2007; Vallius et al., 2005). Ba was added to lubricating oil to prevent engine damage (Kim et al., 2004). NO₂⁻ originated from traffic emissions (Liao & Wu, 2020; Wang et al., 2005). Contributions from the traffic related source rised during peak traffic hours at 8:00-10:00 and 17:00-19:00 (Figure 7).

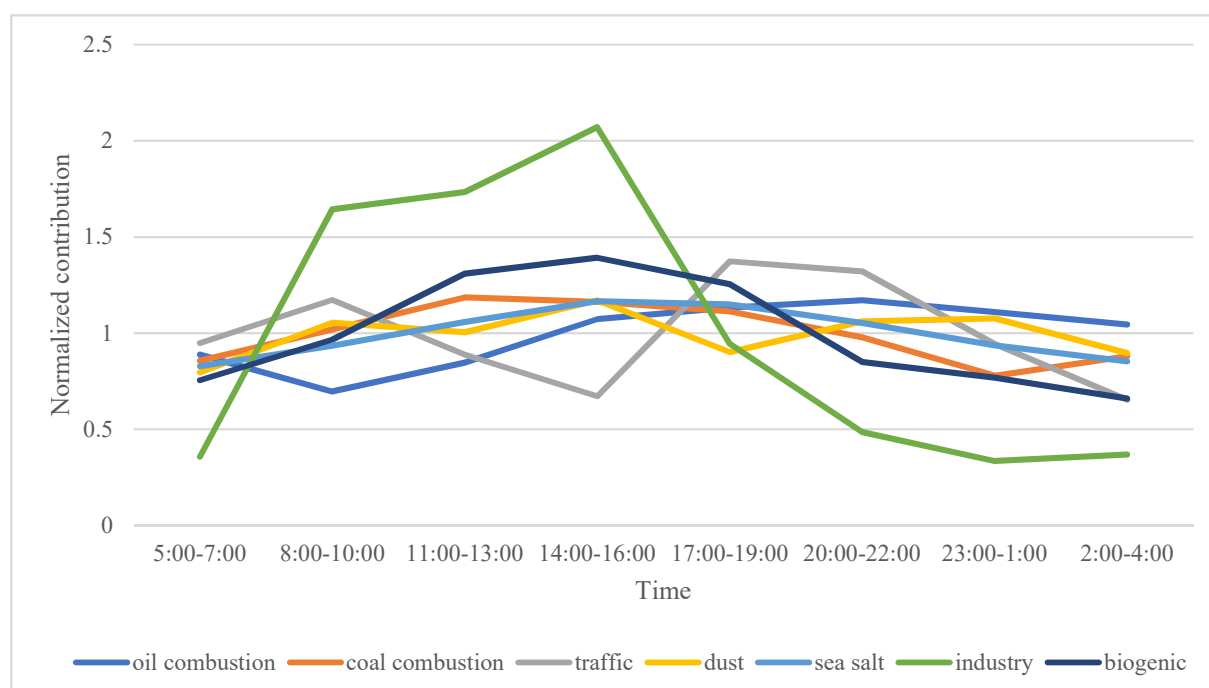
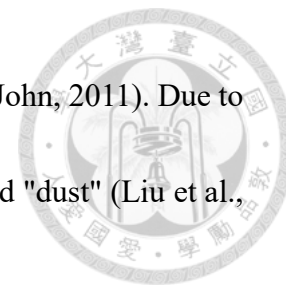


Figure 7 Diurnal plot of Model 2

Factor 2 was characterized by the highest EV of Ca, Ti, and moderate Fe. Ca, Ti, and Fe are primarily crustal elements and are associated with **dust** (Chow et al., 2015; Galvão et al., 2021). Additionally, some literature suggested that Ca and Ti might also

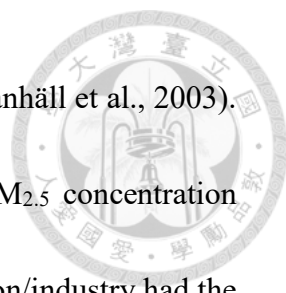
be related to construction activities (Galvão et al., 2021; Karnae & John, 2011). Due to the distinct characteristics of crustal elements, this factor was named "dust" (Liu et al., 2016; Liu et al., 2017) .



Oil combustion was identified by V and Ni. Previous studies have shown that ship engines exhaust contents V and Ni, which are common indicators of oil combustion. The ship engines exhaust was from the burning oil by ships in nearby ports (Gugamsetty et al., 2012; Vallius et al., 2005). Moderate level of NH_4^+ and NO_3^- indicated that this pollution source was related to both combustion and secondary pollution sources. Taipei City has tightened its boiler emission standards since 2017 and gradually phased out fuel boilers. Therefore, fuel-related pollution sources may come from port ship engine emissions or cross-regional transportation.

Coal combustion/industry was characterized by Pb, K, As, Se, Br, NH_4^+ and SO_4^{2-} . Se can be found in coal combustion ash in the form of SeO_2 , which may also be related to coke and steel production facilities (Lee et al., 2008). Br, K, and Pb originated from industrial sources and combustion activities, such as coal burning, metal processing, or smelting (Han et al., 2006). NH_4^+ and SO_4^{2-} indicated secondary ammonium sulfate, which are related to industrial activity emissions and is an indicator of inorganic secondary pollution (Hopke, 1985). Furthermore, the presence of Pb suggested the possibility of long-range transported pollution, which could be associated

with coal combustions and industrial emissions (Hsu et al., 2005; Janhäll et al., 2003).



The contribution of six sources and the reconstructed trend of PM_{2.5} concentration (RPM) are shown in Figure 8. From 2023/1/7 to 1/9, coal combustion/industry had the highest contribution, and the potential source regions of coal combustion/industry can be estimated by using the backward trajectory analysis using HYbrid Single-Particle Lagrangian Integrated Trajectory (HYSPLIT) model developed by National Oceanic and Atmospheric Administration (Draxler & Rolph, 2010). The height could be selected to meet the actual sampling height and the atmosphere above, and the model could simulate the air mass backward trajectory line through calculation based on meteorological condition. A 24-hr HYSPLIT model at the height of 1000 meters above ground level was implemented. It was observed that the backward trajectory of this factor originates from Keelung and eventually traced back to China (Figure 9). Therefore, the pollution of coal combustion/industry was transported from industrial districts of China brought by the northeast monsoon.

Recognized by high EVs of Cr, and Mn, the sixth factor could be associated with **industrial emissions** (Han et al., 2006). Due to the limited number of industrial sources within Taipei City, it is likely that the pollutants originate from various industrial parks located in the surrounding regions (Liao & Wu, 2020; Liao et al., 2017). Na⁺ and Cl⁻ are typical components of sea salt, therefore the last factor was named “**sea salt**” (Lee

et al., 1999; Vallius et al., 2005).



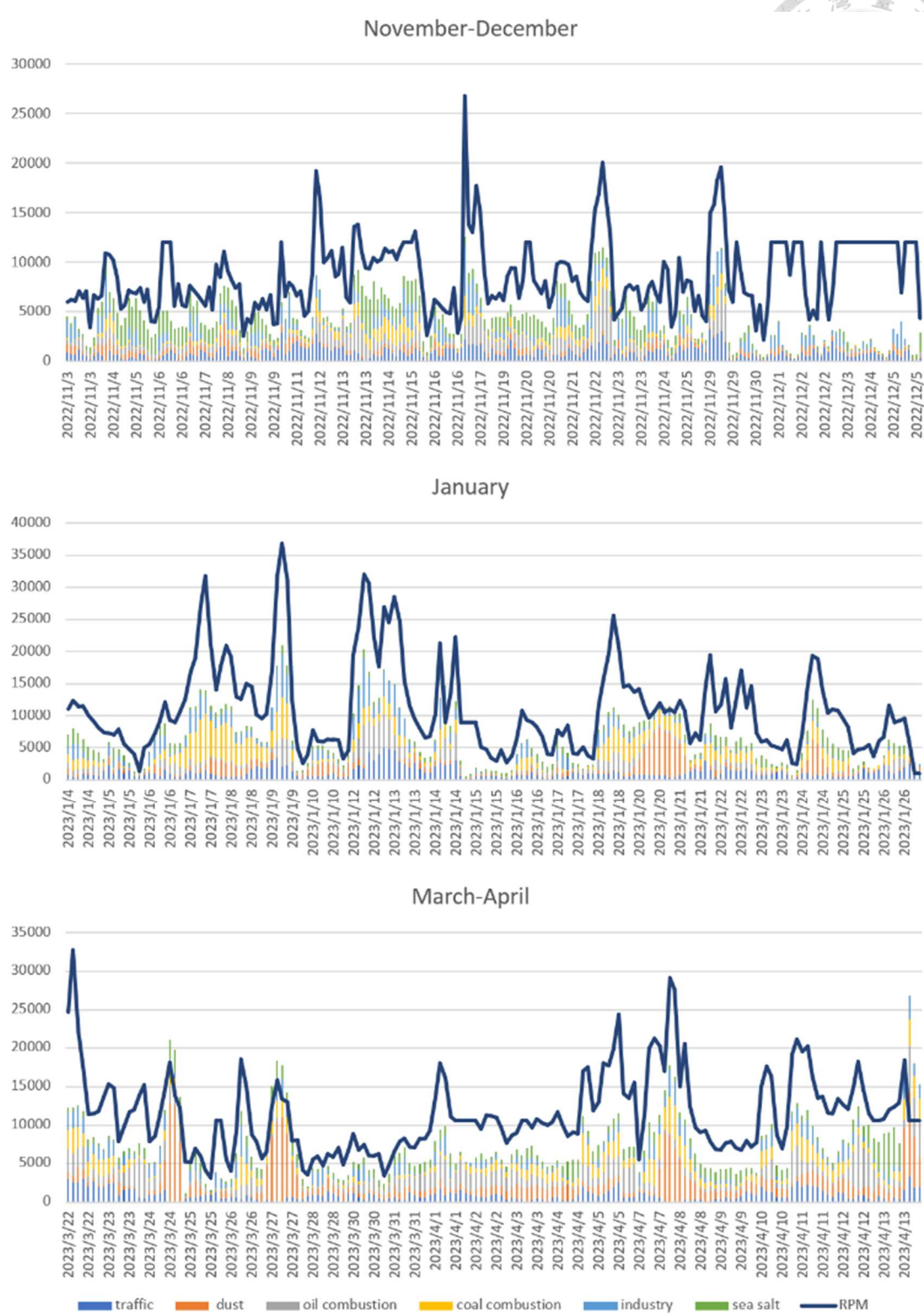


Figure 8 The contribution of six sources and the reconstructed trend of PM_{2.5} concentration (RPM) of Model 1

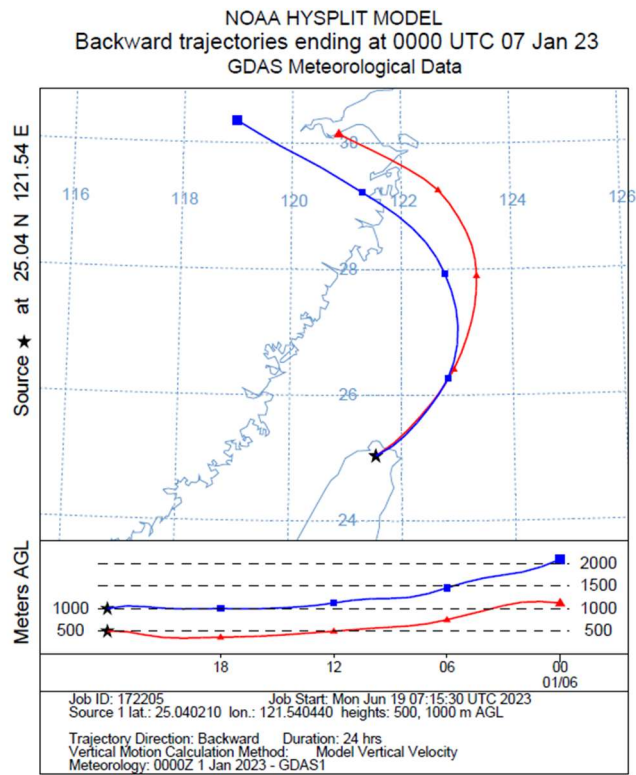
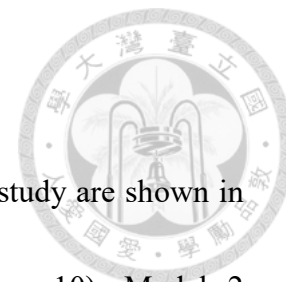


Figure 9 Estimation of the source of coal combustion/industry by backward trajectory HYSPLIT model (24-hour duration)

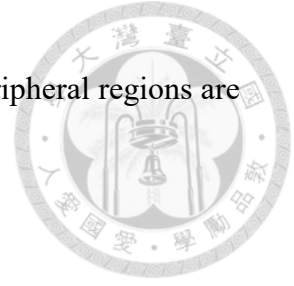
3.2.2. Factor Identification of Model 2



The sources corresponding to the organic compounds in this study are shown in Table 5. After adding organic compounds into analysis (Figure 10), Model 2 additionally identified a pollution source named "Biogenic Source." Characteristic species including 2-MT, arabitol and moderate loading of mannitol. 2-MT is commonly used to trace the SOA formation from isoprene oxidation and primarily originates from biogenic sources (Edney et al., 2005; Ion et al., 2005). Arabitol and mannitol, on the other hand, are the components of fungal spores (Golly et al., 2019). Biogenic pollutants exhibited higher concentrations during daytime and lower concentrations at nighttime. 2-MT is a secondary tracer of isoprene, and it is an important marker for identifying biogenic source. Isoprene undergoes photochemical reactions with NO_x emissions from vehicles and machinery, leading to the formation of 2-MT (El Haddad et al., 2011; García et al., 2017). This process could be a possible reason for the higher daytime contributions observed in Figure 7.

The environments in Taiwan are suitable for fungi to grow, due to the relative humidity higher than 70% and temperature of 20-30 °C (Li & Kuo, 1992). Figure 11 shows that the two peaks of the high contribution of biogenic source occurred at 2022/11/12 and 2023/4/5. The backward trajectory paths primarily originated from the surrounding mountainous areas like Yilan (錯誤! 找不到參照來源。). It is speculated

that the biogenic aerosols from the natural environment in these peripheral regions are transported to the Daan monitoring station.



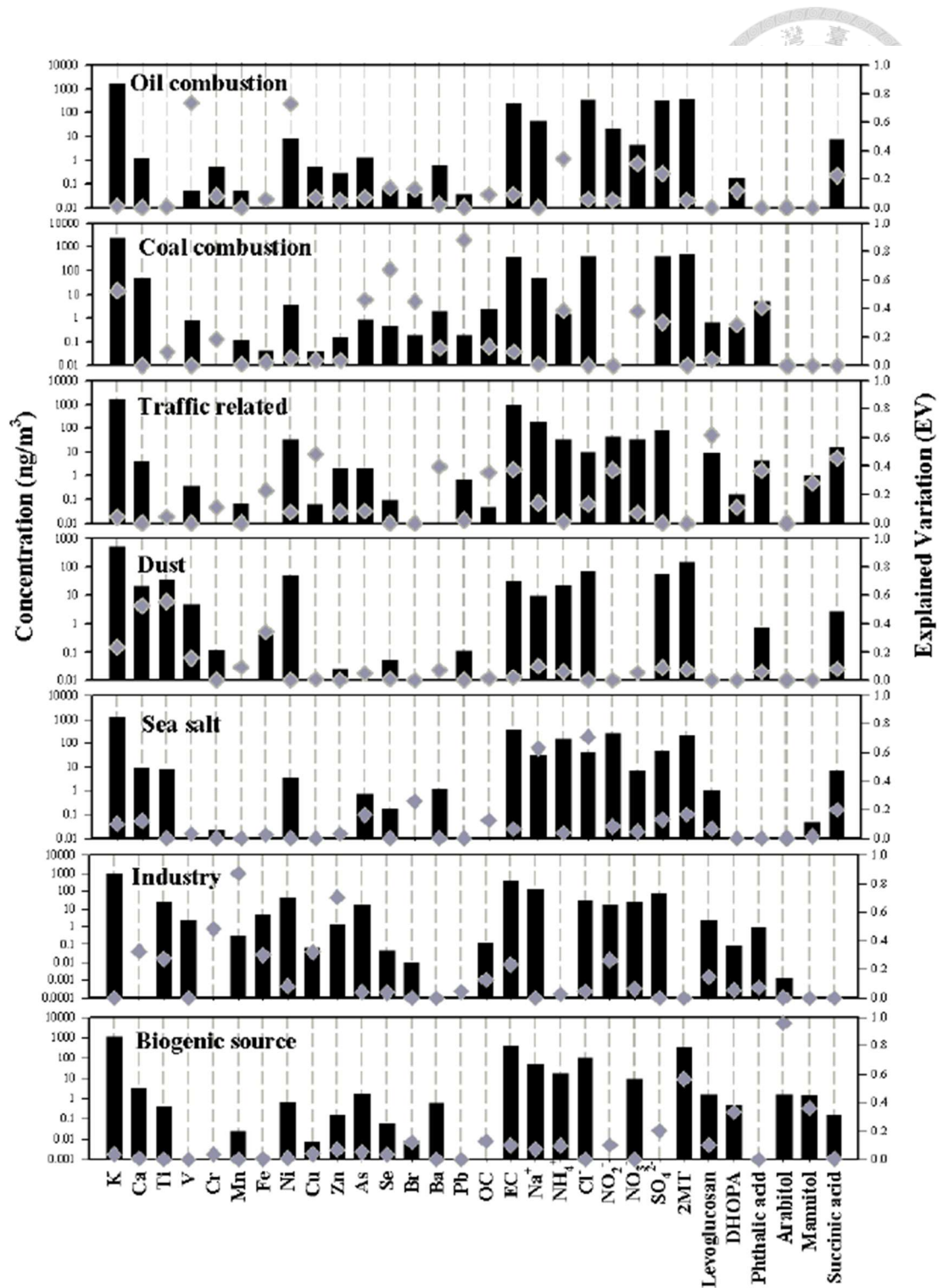
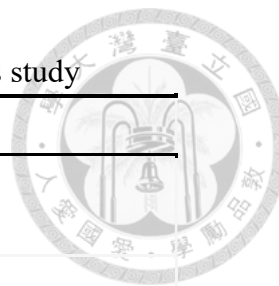


Figure 10 Source profiles of each chemical species of Model 2 (black bars denote concentration; gray points denote explained variation)

Table 5 The sources corresponding to the organic compounds in this study

Compounds	Type	Apportion to ...
2-MT	Secondary (Isoprene)	Biogenic
DHOPA	Secondary (Toluene)	Biogenic Coal combustion/industry
Levogluconan	Primary	Traffic related (+Biomass burning)
Phthalic acid	Secondary (Naphthalene)	Coal combustion/industry Traffic related
Arabitol	Primary	Biogenic
Mannitol	Primary	
Succinic acid	Primary	Traffic related (+Biomass burning)
Cholesterol	Primary	Excluded from the data



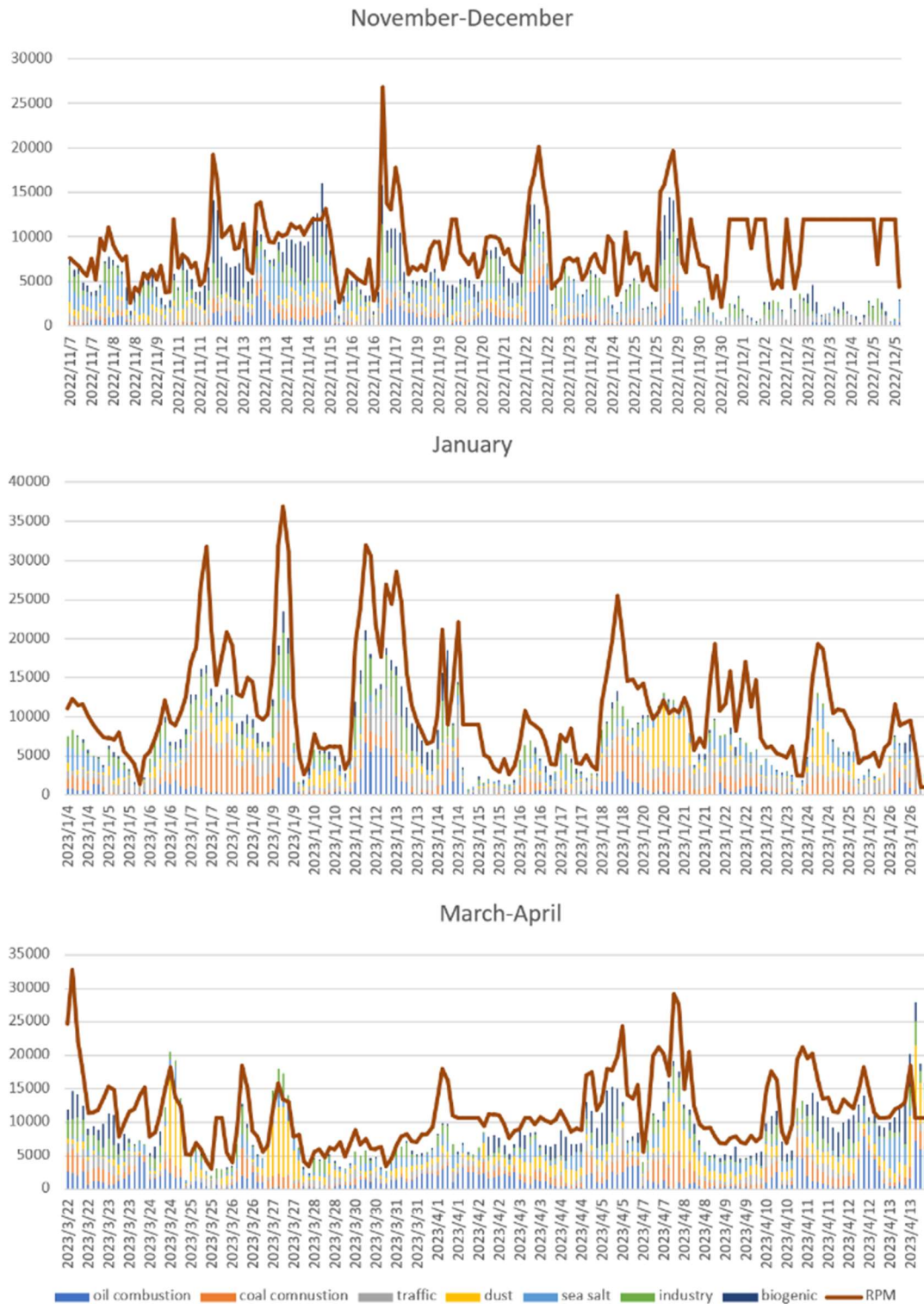


Figure 11 The contribution of six sources and the reconstructed trend of PM_{2.5} concentration (RPM) of Model 2

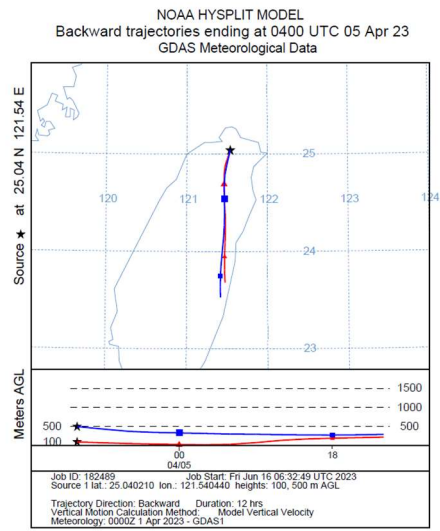
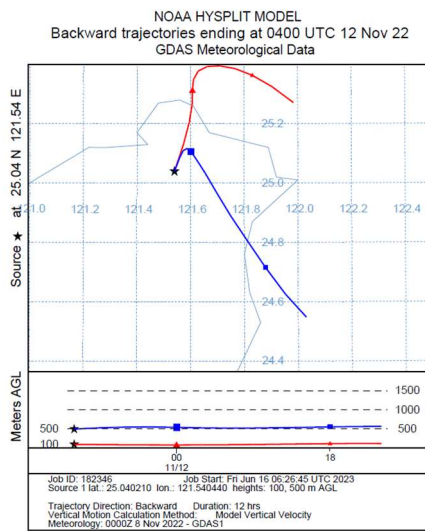
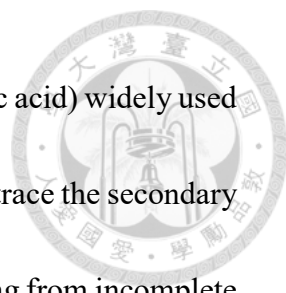


Figure 12 Estimation of the source of biogenic source by backward trajectory
HYSPLIT model (24-hour duration)



Phthalates are diesters of 1,2-benzenedicarboxylic acid (phthalic acid) widely used in industrial applications (Gadi et al., 2019). Phthalic acid is used to trace the secondary organic aerosol (SOA) derived from naphthalene, typically originating from incomplete combustion of carbonaceous materials or industrial use (Wang et al., 2015). It was apportioned to the coal combustion/industry and traffic in the profile of Model 2.

DHOPA is a marker for solvent use, traffic emission, and biomass burning (Ding et al., 2017; Kleindienst et al., 2004; Kleindienst et al., 2007). The EV of DHOPA did not exceed 0.4 in all factor. It might be because of the broad range of the source types. DHOPA is a unique product from the oxidation of toluene in the presence of elevated NO_x (Kleindienst et al., 2007), and it has been identified as a tracer for toluene SOA (Gao et al., 2019). The temporal trend was similar to 2-MT due to the reaction of NO_x in the daytime (Yuan et al., 2018). This might be the reason why moderate EV of DHOPA were apportioned to the biogenic source.

Levoglucosan and succinic acid are common markers of biomass burning (Elias et al., 2001; Urban et al., 2012; Yen et al., 2022). However, levoglucosan and succinic acid were apportioned to traffic related source of Model 2 with moderate loading of OC and EC. It was speculated that this might be because of specific spatial direction and temporal trends of levoglucosan were similar to traffic emissions, causing different pollution sources to be mixed into the same factor. Some studies had found that traffic

related source could mix with biomass burning (Benchrif et al., 2022; Liu et al., 2016).

Potassium element (K) and potassium ion (K^+) were considered as a marker for biomass burning in previous studies (Andreae, 1983; Lewis et al., 1988; Puxbaum et al., 2007; Watson & Chow, 2001). However, in the current study, K has a low correlation with levoglucosan ($=0.18$) (Figure 13) while the data quality of K^+ prevented such a correlation calculation. Although K^+ was regarded as a better marker than K (Lewis et al., 1988; Puxbaum et al., 2007), in Urban et al. (Urban et al., 2012) the authors still showed that some circumstances could cause a strong influence of non-biomass burning sources of K^+ (e.g. from fertilizers), indicating the importance of using levoglucosan as a marker for biomass burning.

Model 2 provided an opportunity to examine the source mixing issue. The correlation between biomass burning markers (levoglucosan and succinic acid) and traffic markers (Cu and Ba) are shown in Figure 14. The data quality of Ba was not high, therefore the value for reference of the correlation was relatively low. The correlation between levoglucosan and Cu was 0.35, supporting the modeling results of retrieving a traffic related factor mixed with biomass burning.

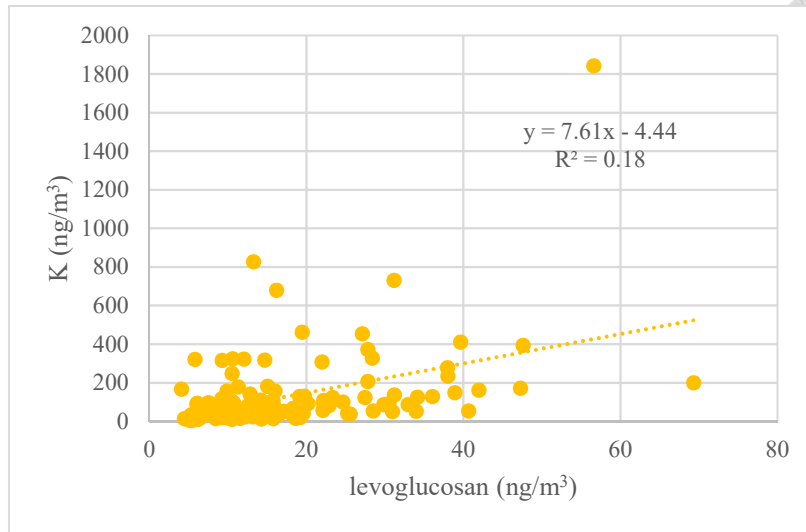


Figure 13 Correlation between levoglucosan and K (after excluded the outliers $R^2=0.15$)

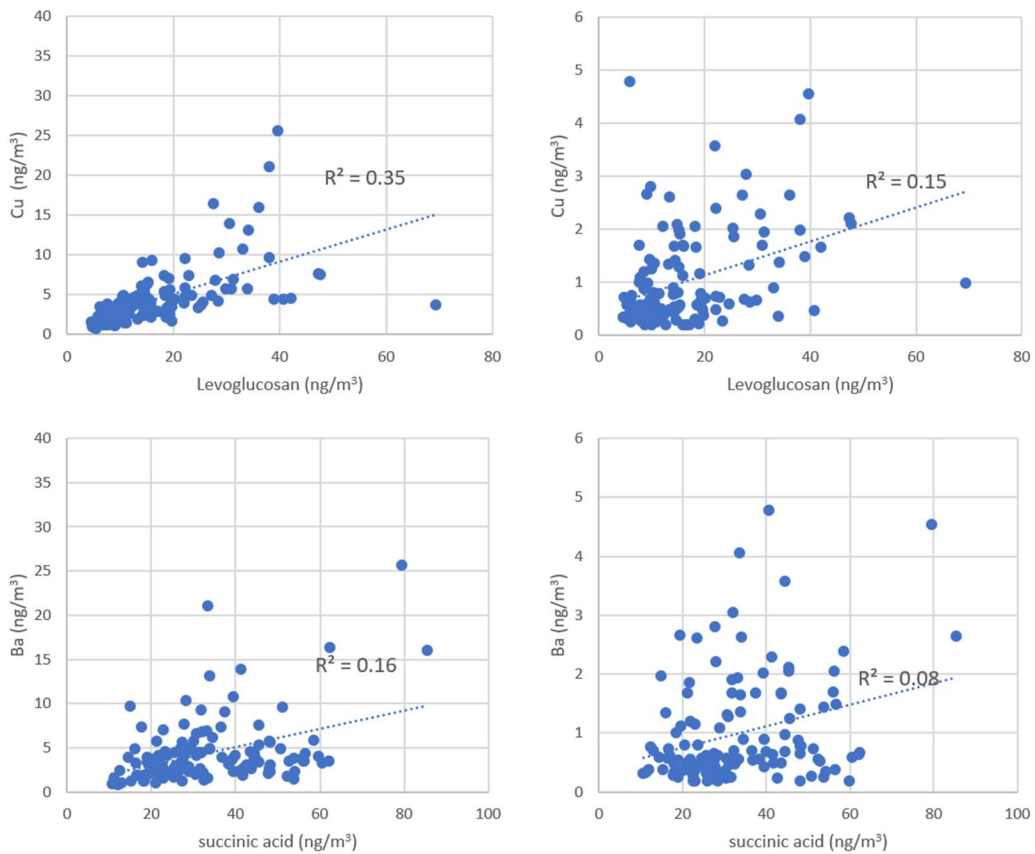
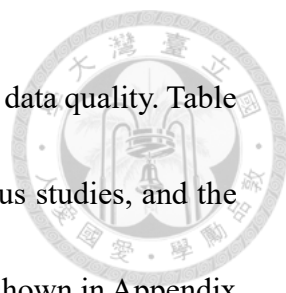


Figure 14 Correlation between biomass burning markers (levoglucosan and succinic acid) and traffic markers (Cu and Ba)

In this study, the number of not detected (ND) concentration of the cholesterol



accounted for 60% of the samples (Figure 15), which lead to the low data quality. Table 5 summarized the concentrations of cholesterol measured in previous studies, and the concentration ranged between ND-6.3 ng/m³ (other compounds are shown in Appendix 7). Source apportionment research showed that cholesterol appears to be one of the most useful tracers for meat smoke (He et al., 2004). Therefore, the concentration of cholesterol could differ from each country due to their cooking styles. Before the main field campaign of this study, a pilot test sampling was conducted at a restaurant ventilator, where the cooking exhaust gathered and released into the atmosphere. The concentrations of cholesterol ranged between 0.6-3.7 ng/m³. In the current study, the average concentration of cholesterol was 0.37, and the concentration ranged between ND-1.95 ng/m³.

Table 5 Atmosphere concentrations of cholesterol of previous studies

studies	Study site	Sampling time (hour)	concentration (ng/m ³)
This study	Taipei, Taiwan	12	ND-1.95
(Islam et al., 2020)	Kathmandu Valley, Nepal	24	ND-2.9
(Schauer et al., 1996)	Los Angeles	24	1.9-2.7
(Fine et al., 2004)	Los Angeles	3.5	ND-3
(Robinson et al., 2006)	Pittsburgh, Pennsylvania	24	0.5-2.5
(Wang et al., 2009)	Beijing, China	12	2.0-5.0
(He et al., 2006)	Beijing, China	24	0.05-6.3
(Omar et al., 2007)	Kuala Lumpur, Malaysia	24(urban) 48(rural)	ND-3.7



3.2.3. Seasonal variation

The contributions of each factor in the three seasons are shown in Figure 16. The contribution of coal combustion/industry was relatively high in winter compared to the other two seasons. It could be observed that the backward trajectory of this factor originated from Keelung and eventually traced back to China (Figure 8). According to Taiwan EPA, during the northeast monsoon, the southward intrusion of continental cold high-pressure systems, or when high-pressure systems move offshore, the wind direction near Taiwan often became northerly or northeasterly. Such wind directions prevailed during the winter, and the wind intensity was relatively stronger. When foreign pollutants accompanied the northeast winds and moved into Taiwan, areas that were originally well-ventilated may experience high concentrations of air pollution (https://airtw.epa.gov.tw/cht/Encyclopedia/pedia02/pedia2_1.aspx).

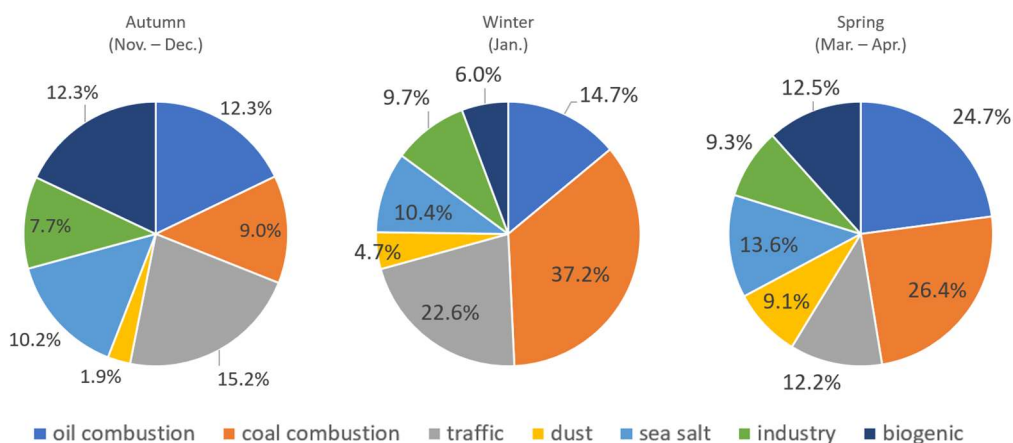


Figure 16 Factor contribution of three seasons

The contribution of oil combustion increased in spring. Figure 10 shows that



there was a consistent contribution of oil combustion from 2023/3/31 to 2023/4/1. A 24-hour HYSPLIT model at the height of 500 and 1000 meters above ground level was executed. It can be observed that the backward trajectory of this factor originates from Keelung Port and Taipei Port. The contributions of biogenic source in this study were 12.3%, 6.0%, and 12.5%, comparable to the values (4% to 14%) reported in previous studies (Table 6) (Khan et al., 2021; Shin et al., 2022; Waked et al., 2014).

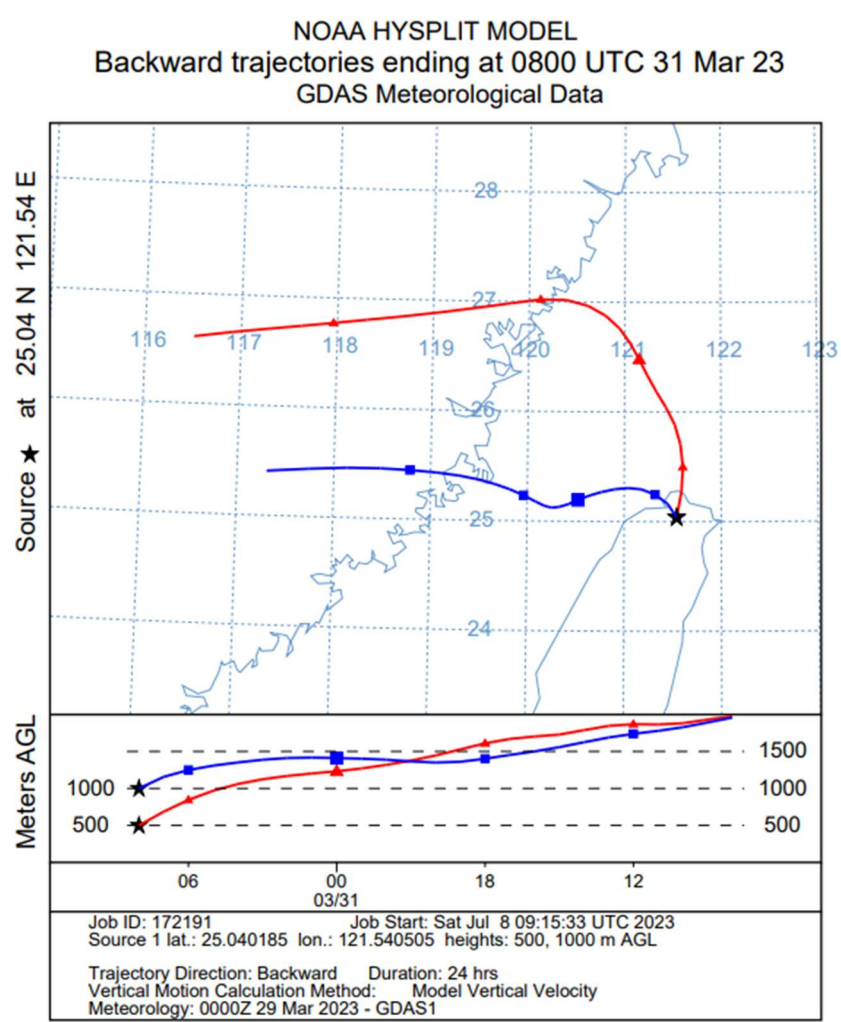


Figure 17 Estimation of the source of oil combustion source by backward trajectory HYSPLIT model (24-hour duration)

Table 6 Summary of contributions of biogenic source in previous study

Reference	Region	Contributions of biogenic source	Season
This study	Taipei, Taiwan	12.3% 6.0% 12.5%	Autumn Winter Spring
(Khan et al., 2021)	Tianjin, China	14%	Summer
(Shin et al., 2022)	Seoul, Korea	4%	The hole year
(Waked et al., 2014)	Lens, France	9%	Spring

The traffic related source was relatively high during winter (Figure 16). During winter in Taipei, the cooling effect near the Earth's surface, known as radiative cooling, leads to lower temperatures. As a result, the temperature increased with altitude. Cold air accumulating near the ground lead to a phenomenon known as the "inversion layer", and this phenomenon was strengthened by the Taipei basin (Chang & Lee, 2007; Chou et al., 2007). The lack of vertical convection due to limited air circulation leads to the accumulation of pollutants, resulting in poorer air quality (Tsuang & Chao, 1999). Another reason for the higher traffic levels in winter was because biomass burning was apportioned in traffic source. Usually the contribution of biomass burning was relatively higher in winter (Song et al., 2007). In present study, the average concentration of levoglucosan (marker of biomass burning) of winter was 20.75 ng/m³, which was higher than the concentration in autumn (15.34 ng/m³) and spring (15.40 ng/m³).



The traffic contribution was lower than expected as an urban site like Taipei (12.2%, 15.2%, and 22.6%). This phenomenon could be attributed to the vertical gradient (Ho et al., 2015; Shi et al., 2012). In Liao et al. (2017), data obtained from various nearby ground-level monitors indicates twice the levels of traffic-related pollutants (such as carbon monoxide, non-methane hydrocarbons, and nitrogen oxides) in comparison to those observed at the study site (Liao et al., 2017). The average concentration of traffic-related pollutants in this study and those measured by nearby ground-level monitor are shown in Table 7. The concentrations measured by ground-level monitor were higher than Daan station in the study months. On the other hand, from the profile of Model 2, it can be observed that SO_4^{2-} and NO_3^- were low, indicating the possibility of being attributed to other sources.

Table 7 The average concentration of traffic-related pollutants in this study and those measured by nearby ground-level monitor (ppm)


Monitor station	CO ¹	NMHC ²	NO ³
ground-level monitor (Datong station)	0.69	0.18	17.79
This study (Daan station)	0.57	0.15	1.78

¹carbon monoxide (CO)

²non-methane hydrocarbons (NMHC)

³nitrogen oxides (NO)

The previous study of source apportionment in Wanhua Taipei collected hourly VOC concentrations and 24-hour PM_{2.5} samples for elemental, water-soluble ions and



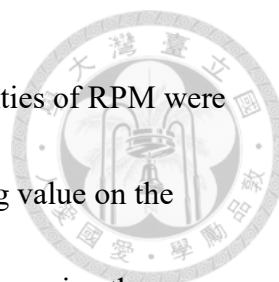
OC/EC. The study showed that secondary aerosol/long-range transport was the largest contributor to PM_{2.5} (Liao et al., 2017). Another study located in Chongcheng Taipei has identified NH₄⁺ as the primary contributor by using hourly measurements of PM_{2.5} components. This finding suggests that NH₄⁺ may originate from local sources or be transported as secondary aerosol (Liao & Wu, 2020). Sulfates and combustion emissions are the dominant factors in the concentration of air pollutants in Banqiao (李崇德 et al., 2018), and this trend remained consistent throughout all seasons.

A secondary aerosol source was not an individual factor in this study, but the marker of secondary aerosol, including SO₄²⁻ and NH₄⁺, were apportioned into “coal combustion/industry” moderately. The coal combustion/industry of this study was from long-range transport (Figure 8), and this result is similar to the study in Wanhua Taipei that the secondary aerosol and long-range transport were mixed in one factor (Liao et al., 2017).

3.3. Sensitivity analysis

The proportion of unidentified of Model 1 and Model 2 is 8.75% and 8.86%, respectively (Figure 18). The R² of predicted and RPM were 0.595 and 0.625, respectively. Adding organic compounds slightly improved the prediction of PM_{2.5}, but it was helpful of separation of the potential sources, such as the biogenic source.

Using the reconstructed PM_{2.5} might cause the total PM_{2.5} become too high due



to the missing value replaced by the median. Although the uncertainties of RPM were set as three times of original uncertainties, and the impact of missing value on the model was neglectable, a sensitivity analysis test was conducted to examine the influence of missing value, by removing the series of missing RPM data that lasted over 5 days. The proportion of unidentified dropped to 4% after removing data of December 1-5 (Figure 10). This test represented the limitation of using RPM as total PM_{2.5}. Removing missing values to a certain extent is necessary to obtain an accurate "unidentified" ratio. Therefore, when using this method in the future, it is important to be mindful of the missing value.

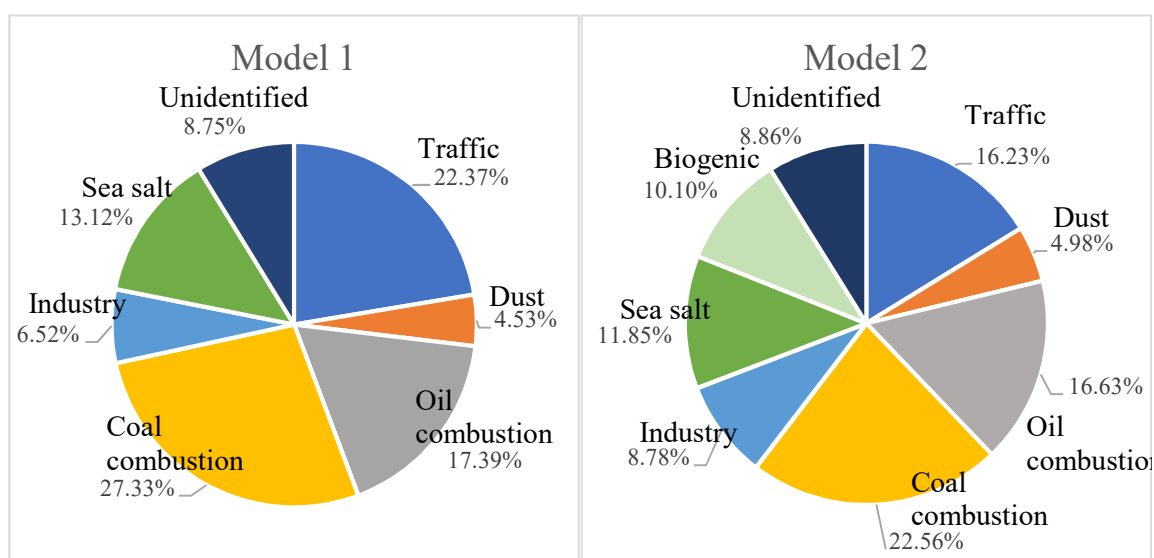
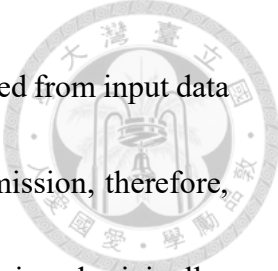


Figure 18 Proportion of the source contribution

3.4. Limitations

There are several limitations in this study:

- (1) Background concentrations of cholesterol were low, which cause the




difficulties in UPLC-MS/MS analyzing. Cholesterol had to be removed from input data due to its poor data quality. It is known as a marker for cooking emission, therefore, this study could not identify cooking emission source as the study designed originally.

(2) To highlight the organic compounds in the model, the hourly data were averaged into 3-hour data. The high time resolution data had been sacrificed for enhancing the importance of low time resolution (organic markers). It is suggested to consider increasing the frequency of manual sampling to enhance temporal resolution in the future study, extending the weighting of organic components in the model calculations.

(3) The replacement of missing values in this study was the median of each season. However, there were other methods to obtain values that could reflect reality. For example, using linear interpolation instead of the median for the missing values could be more suitable for hourly data. Replacing measured $PM_{2.5}$ with reconstructed $PM_{2.5}$ might lead to some issues that did not encounter before, such as missing values replaced by the median could cause inconsistent with reality.

(4) The traffic contribution was lower than expected as an urban site like Taipei (12.2%, 15.2%, and 22.6%). From the profile of Model 2, it can be observed that NO_3^- were low, indicating the possibility of being attributed to other sources of contamination.

(5) In this study, there was a possibility of overestimation in the contribution from



biogenic sources. Firstly, biogenic sources lack other supporting identifying components. Secondly, DHOPA was apportioned into the biogenic source. It was possible that some combustion sources have been apportioned to biogenic sources, leading to an overestimation.

Chapter 4 Conclusions and recommendations

The sources of PM_{2.5} are highly complex, and the three online monitoring instruments at the Daan station can not measure organic markers that are useful for identifying sources. This imposes certain limitations on identifying the sources of organic aerosol pollution. This study improved upon the limitations of the existing monitoring instruments by analyzing specific organic components, including 2-MT, DHOPA, levoglucosan, phthalic acid, succinic acid, arabitol, and mannitol. Through the analysis of organic compounds, this study further differentiated and identified the sources.

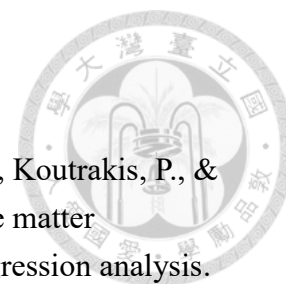
From the results of Model 2, it can be observed that after incorporating organic components, the PMF model can resolve a "biogenic source" with indicator species such as 2-MT and arabitol. This source was not previously identified in the field studies conducted in Taipei (Ho et al., 2018; Huang et al., 2022; Liao & Wu, 2020), and this finding highlighted the improvement of PMF performance by involving organic

components. Furthermore, the backward trajectory model suggested that this pollution source originated from the surrounding natural environment.




For future improvement of the PMF analysis, it is suggested to consider increasing the frequency of manual sampling to enhance the temporal resolution and extend the weighting of organic components in the model calculations. Furthermore, it could be more persuasive by increasing the sample size in the model inputs, or including the summer samples. These steps can further enhance the resolution and accuracy of PMF analysis. For the cholesterol analysis, other methods are suggested, such as using nitrogen evaporators to concentrate the samples.

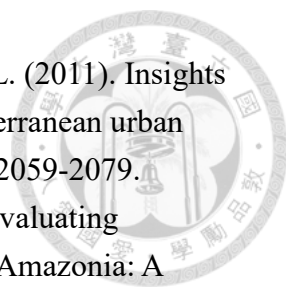
Due to geographical location of Taipei, air pollution in Taipei City is influenced not only by domestic emission sources but also by transboundary transport, leading to poor air quality during specific time periods. However, in terms of control strategies, it is still necessary to focus on domestic pollution sources. This study provides a scientific basis for future consideration and regulation of pollutions in Taipei. According to the pollution source analysis conducted in this project during winter, the identified pollution source categories also include local sources such as traffic, oil combustion, dust, and biogenic source. Therefore, it is necessary to strengthen control measures for local pollution sources during winter.

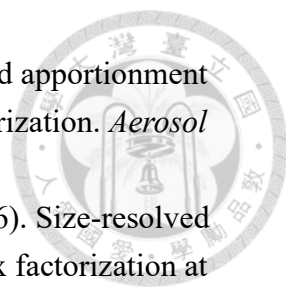


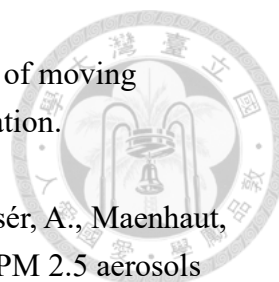
References

- Achilleos, S., Kioumourtzoglou, M.-A., Wu, C.-D., Schwartz, J. D., Koutrakis, P., & Papatheodorou, S. I. (2017). Acute effects of fine particulate matter constituents on mortality: A systematic review and meta-regression analysis. *Environment international*, *109*, 89-100.
- Akhtar, J., Idris, A., & Abd. Aziz, R. (2014). Recent advances in production of succinic acid from lignocellulosic biomass. *Applied microbiology and biotechnology*, *98*, 987-1000.
- Albinet, A., Lanzafame, G. M., Srivastava, D., Bonnaire, N., Nalin, F., & Wise, S. A. (2019). Analysis and determination of secondary organic aerosol (SOA) tracers (markers) in particulate matter standard reference material (SRM 1649b, urban dust). *Analytical and Bioanalytical Chemistry*, *411*(23), 5975-5983. <https://doi.org/10.1007/s00216-019-02015-6>
- Almeida, S., Manousakas, M., Diapouli, E., Kertesz, Z., Samek, L., Hristova, E., Šega, K., Alvarez, R. P., Belis, C., & Eleftheriadis, K. (2020). Ambient particulate matter source apportionment using receptor modelling in European and Central Asia urban areas. *Environmental Pollution*, *266*, 115199.
- Andreae, M. O. (1983). Soot carbon and excess fine potassium: Long-range transport of combustion-derived aerosols. *Science*, *220*(4602), 1148-1151.
- Anttila, P., Paatero, P., Tapper, U., & Järvinen, O. (1995). Source identification of bulk wet deposition in Finland by positive matrix factorization. *Atmospheric environment*, *29*(14), 1705-1718.
- Bauer, H., Claeys, M., Vermeylen, R., Schueller, E., Weinke, G., Berger, A., & Puxbaum, H. (2008). Arabitol and mannitol as tracers for the quantification of airborne fungal spores. *Atmospheric environment*, *42*(3), 588-593.
- Bauer, J. J., Yu, X.-Y., Cary, R., Laulainen, N., & Berkowitz, C. (2009). Characterization of the sunset semi-continuous carbon aerosol analyzer. *Journal of the Air & Waste Management Association*, *59*(7), 826-833.
- Benchrif, A., Tahri, M., Guinot, B., Chakir, E. M., Zahry, F., Baghdad, B., Bounakhla, M., Cachier, H., & Costabile, F. (2022). Aerosols in Northern Morocco-2: Chemical Characterization and PMF Source Apportionment of Ambient PM_{2.5}. *Atmosphere*, *13*(10), 1701.
- Bhatarai, H., Saikawa, E., Wan, X., Zhu, H., Ram, K., Gao, S., Kang, S., Zhang, Q., Zhang, Y., & Wu, G. (2019). Levoglucosan as a tracer of biomass burning: Recent progress and perspectives. *Atmospheric Research*, *220*, 20-33.
- Chan, M. N., Choi, M. Y., Ng, N. L., & Chan, C. K. (2005). Hygroscopicity of water-soluble organic compounds in atmospheric aerosols: Amino acids and biomass

- 
- burning derived organic species. *Environmental Science & Technology*, 39(6), 1555-1562.
- Chang, S.-C., & Lee, C.-T. (2007). Evaluation of the trend of air quality in Taipei, Taiwan from 1994 to 2003. *Environmental monitoring and assessment*, 127, 87-96.
- Chen, L. C., & Lippmann, M. (2009). Effects of metals within ambient air particulate matter (PM) on human health. *Inhalation toxicology*, 21(1), 1-31.
- Chou, C. C.-K., Lee, C.-T., Chen, W.-N., Chang, S.-Y., Chen, T.-K., Lin, C.-Y., & Chen, J.-P. (2007). Lidar observations of the diurnal variations in the depth of urban mixing layer: a case study on the air quality deterioration in Taipei, Taiwan. *Science of the Total Environment*, 374(1), 156-166.
- Chou, T.-I. (2021). *Integrate Continuous Monitoring and Manual Sampling Data to Perform Source Apportionment of PM_{2.5} with Modified Receptor Model in Taichung Metropolis during Springtime* National Taiwan University].
- Chow, J. C., Lowenthal, D. H., Chen, L.-W. A., Wang, X., & Watson, J. G. (2015). Mass reconstruction methods for PM 2.5: a review. *Air Quality, Atmosphere & Health*, 8, 243-263.
- Crespi, A., Bernardoni, V., Calzolari, G., Lucarelli, F., Nava, S., Valli, G., & Vecchi, R. (2016). Implementing constrained multi-time approach with bootstrap analysis in ME-2: An application to PM_{2.5} data from Florence (Italy). *Science of the Total Environment*, 541, 502-511.
- Dai, Y., Chang, H. J., Cao, S. X., Liu, D. Y., Xu, X. L., & Zhou, G. H. (2011). Nonvolatile taste compounds in cooked Chinese Nanjing duck meat following postproduction heat treatment. *Journal of food science*, 76(5), C674-C679.
- Ding, X., Zhang, Y.-Q., He, Q.-F., Yu, Q.-Q., Wang, J.-Q., Shen, R.-Q., Song, W., Wang, Y.-S., & Wang, X.-M. (2017). Significant increase of aromatics-derived secondary organic aerosol during fall to winter in China. *Environmental Science & Technology*, 51(13), 7432-7441.
- Draxler, R., & Rolph, G. (2010). HYSPLIT (HYbrid Single-Particle Lagrangian Integrated Trajectory) model access via NOAA ARL READY website (<http://ready.arl.noaa.gov/HYSPLIT.php>), NOAA Air Resources Laboratory. Silver Spring, MD, 25(1).
- Edney, E., Kleindienst, T., Jaoui, M., Lewandowski, M., Offenber, J., Wang, W., & Claeys, M. (2005). Formation of 2-methyl tetrols and 2-methylglyceric acid in secondary organic aerosol from laboratory irradiated isoprene/NO_x/SO₂/air mixtures and their detection in ambient PM_{2.5} samples collected in the eastern United States. *Atmospheric environment*, 39(29), 5281-5289.
- El Haddad, I., Marchand, N., Temime-Roussel, B., Wortham, H., Piot, C., Besombes,

- 
- J.-L., Baduel, C., Voisin, D., Armengaud, A., & Jaffrezo, J.-L. (2011). Insights into the secondary fraction of the organic aerosol in a Mediterranean urban area: Marseille. *Atmospheric Chemistry and Physics*, 11(5), 2059-2079.
- Elias, V. O., Simoneit, B. R., Cordeiro, R. C., & Turcq, B. (2001). Evaluating levoglucosan as an indicator of biomass burning in Carajas, Amazonia: A comparison to the charcoal record. *Geochimica et Cosmochimica Acta*, 65(2), 267-272.
- Falkovich, A., Graber, E., Schkolnik, G., Rudich, Y., Maenhaut, W., & Artaxo, P. (2005). Low molecular weight organic acids in aerosol particles from Rondônia, Brazil, during the biomass-burning, transition and wet periods. *Atmospheric Chemistry and Physics*, 5(3), 781-797.
- Fine, P. M., Chakrabarti, B., Krudysz, M., Schauer, J. J., & Sioutas, C. (2004). Diurnal variations of individual organic compound constituents of ultrafine and accumulation mode particulate matter in the Los Angeles basin. *Environmental Science & Technology*, 38(5), 1296-1304.
- Gadi, R., Sharma, S. K., & Mandal, T. K. (2019). Source apportionment and health risk assessment of organic constituents in fine ambient aerosols (PM_{2.5}): a complete year study over National Capital Region of India. *Chemosphere*, 221, 583-596.
- Galvão, E. S., de Cassia Feroni, R., & Orlando, M. T. D. A. (2021). A review of the main strategies used in the interpretation of similar chemical profiles yielded by receptor models in the source apportionment of particulate matter. *Chemosphere*, 269, 128746.
- Gao, J., Peng, X., Chen, G., Xu, J., Shi, G.-L., Zhang, Y.-C., & Feng, Y.-C. (2016). Insights into the chemical characterization and sources of PM_{2.5} in Beijing at a 1-h time resolution. *Science of the Total Environment*, 542, 162-171.
- Gao, Y., Wang, H., Zhang, X., Jing, S. a., Peng, Y., Qiao, L., Zhou, M., Huang, D. D., Wang, Q., & Li, X. (2019). Estimating secondary organic aerosol production from toluene photochemistry in a megacity of China. *Environmental Science & Technology*, 53(15), 8664-8671.
- García, M. I., Van Drooge, B. L., Rodríguez, S., & Alastuey, A. (2017). Speciation of organic aerosols in the Saharan Air Layer and in the free troposphere westerlies. *Atmospheric Chemistry and Physics*, 17(14), 8939-8958.
- Golly, B., Waked, A., Weber, S., Samake, A., Jacob, V., Conil, S., Rangognio, J., Chrétien, E., Vagnot, M.-P., & Robic, P.-Y. (2019). Organic markers and OC source apportionment for seasonal variations of PM_{2.5} at 5 rural sites in France. *Atmospheric environment*, 198, 142-157.
- Gugamsetty, B., Wei, H., Liu, C.-N., Awasthi, A., Hsu, S.-C., Tsai, C.-J., Roam, G.-D.,

- 
- Wu, Y.-C., & Chen, C.-F. (2012). Source characterization and apportionment of PM₁₀, PM_{2.5} and PM_{0.1} by using positive matrix factorization. *Aerosol and Air Quality Research*, 12(4), 476-491.
- Han, J., Moon, K., Lee, S., Kim, Y., Ryu, S., Cliff, S., & Yi, S. (2006). Size-resolved source apportionment of ambient particles by positive matrix factorization at Gosan background site in East Asia. *Atmospheric Chemistry and Physics*, 6(1), 211-223.
- He, L.-Y., Hu, M., Huang, X.-F., Yu, B.-D., Zhang, Y.-H., & Liu, D.-Q. (2004). Measurement of emissions of fine particulate organic matter from Chinese cooking. *Atmospheric environment*, 38(38), 6557-6564.
- He, L.-Y., Hu, M., Huang, X.-F., Zhang, Y.-H., & Tang, X.-Y. (2006). Seasonal pollution characteristics of organic compounds in atmospheric fine particles in Beijing. *Science of the Total Environment*, 359(1-3), 167-176.
- Heo, J., Dulger, M., Olson, M. R., McGinnis, J. E., Shelton, B. R., Matsunaga, A., Sioutas, C., & Schauer, J. J. (2013). Source apportionments of PM_{2.5} organic carbon using molecular marker Positive Matrix Factorization and comparison of results from different receptor models. *Atmospheric environment*, 73, 51-61.
- Ho, C.-C., Chan, C.-C., Cho, C.-W., Lin, H.-I., Lee, J.-H., & Wu, C.-F. (2015). Land use regression modeling with vertical distribution measurements for fine particulate matter and elements in an urban area. *Atmospheric environment*, 104, 256-263.
- Ho, W.-Y., Tseng, K.-H., Liou, M.-L., Chan, C.-C., & Wang, C.-h. (2018). Application of positive matrix factorization in the identification of the sources of PM_{2.5} in Taipei City. *International journal of environmental research and public health*, 15(7), 1305.
- Hopke, P. K. (1985). *Receptor modeling in environmental chemistry*. John Wiley & Sons.
- Hopke, P. K. (2016). Review of receptor modeling methods for source apportionment. *Journal of the Air & Waste Management Association*, 66(3), 237-259.
- Hsu, S.-C., Liu, S. C., Jeng, W.-L., Lin, F.-J., Huang, Y.-T., Lung, S.-C. C., Liu, T.-H., & Tu, J.-Y. (2005). Variations of Cd/Pb and Zn/Pb ratios in Taipei aerosols reflecting long-range transport or local pollution emissions. *Science of the Total Environment*, 347(1-3), 111-121.
- Hu, D., Bian, Q., Lau, A. K., & Yu, J. Z. (2010). Source apportioning of primary and secondary organic carbon in summer PM_{2.5} in Hong Kong using positive matrix factorization of secondary and primary organic tracer data. *Journal of Geophysical Research: Atmospheres*, 115(D16).
- Huang, C.-S., Liao, H.-T., Lu, S.-H., Chan, C.-C., & Wu, C.-F. (2022). Identifying and



quantifying PM_{2.5} pollution episodes with a fusion method of moving window technique and constrained Positive Matrix Factorization. *Environmental Pollution*, 120382.

Ion, A., Vermeylen, R., Kourtchev, I., Cafmeyer, J., Chi, X., Gelencsér, A., Maenhaut, W., & Claeys, M. (2005). Polar organic compounds in rural PM_{2.5} aerosols from K-puszta, Hungary, during a 2003 summer field campaign: Sources and diel variations. *Atmospheric Chemistry and Physics*, 5(7), 1805-1814.

Islam, M. R., Jayarathne, T., Simpson, I. J., Werden, B., Maben, J., Gilbert, A., Praveen, P. S., Adhikari, S., Panday, A. K., & Rupakheti, M. (2020). Ambient air quality in the Kathmandu Valley, Nepal, during the pre-monsoon: concentrations and sources of particulate matter and trace gases. *Atmospheric Chemistry and Physics*, 20(5), 2927-2951.

Janhäll, S., Molnár, P., & Hallquist, M. (2003). Vertical distribution of air pollutants at the Gustavii Cathedral in Göteborg, Sweden. *Atmospheric environment*, 37(2), 209-217.

Jiménez, E., Linares, C., Rodríguez, L., Bleda, M., & Díaz, J. (2009). Short-term impact of particulate matter (PM_{2.5}) on daily mortality among the over-75 age group in Madrid (Spain). *Science of the Total Environment*, 407(21), 5486-5492.

Karnae, S., & John, K. (2011). Source apportionment of fine particulate matter measured in an industrialized coastal urban area of South Texas. *Atmospheric environment*, 45(23), 3769-3776.

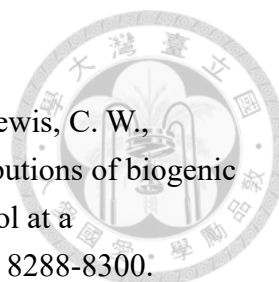
Keim, B. D., Meeker, L. D., & Slater, J. F. (2005). Manual synoptic climate classification for the East Coast of New England (USA) with an application to PM_{2.5} concentration. *Climate Research*, 28(2), 143-153.

Kelly, F. J., & Fussell, J. C. (2012). Size, source and chemical composition as determinants of toxicity attributable to ambient particulate matter. *Atmospheric environment*, 60, 504-526.

Khan, J. Z., Sun, L., Tian, Y., Shi, G., & Feng, Y. (2021). Chemical characterization and source apportionment of PM₁ and PM_{2.5} in Tianjin, China: Impacts of biomass burning and primary biogenic sources. *Journal of Environmental Sciences*, 99, 196-209.


Kim, E., Hopke, P. K., & Edgerton, E. S. (2004). Improving source identification of Atlanta aerosol using temperature resolved carbon fractions in positive matrix factorization. *Atmospheric environment*, 38(20), 3349-3362.

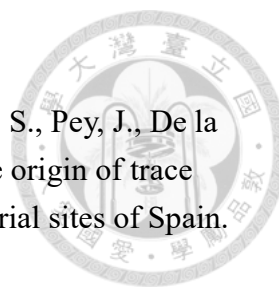
Kleindienst, T., Conner, T., McIver, C., & Edney, E. (2004). Determination of secondary organic aerosol products from the photooxidation of toluene and their implications in ambient PM_{2.5}. *Journal of Atmospheric Chemistry*, 47,



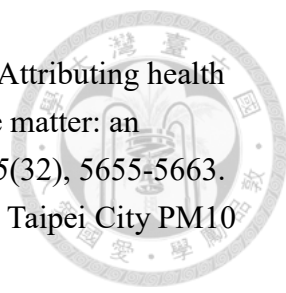
79-100.

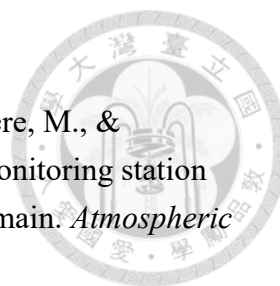
- Kleindienst, T. E., Jaoui, M., Lewandowski, M., Offenberg, J. H., Lewis, C. W., Bhave, P. V., & Edney, E. O. (2007). Estimates of the contributions of biogenic and anthropogenic hydrocarbons to secondary organic aerosol at a southeastern US location. *Atmospheric environment*, *41*(37), 8288-8300.
- Kuo, C.-P., Liao, H.-T., Chou, C. C.-K., & Wu, C.-F. (2014). Source apportionment of particulate matter and selected volatile organic compounds with multiple time resolution data. *Science of the Total Environment*, *472*, 880-887.
- Lee, E., Chan, C. K., & Paatero, P. (1999). Application of positive matrix factorization in source apportionment of particulate pollutants in Hong Kong. *Atmospheric environment*, *33*(19), 3201-3212.
- Lee, S., Liu, W., Wang, Y., Russell, A. G., & Edgerton, E. S. (2008). Source apportionment of PM_{2.5}: Comparing PMF and CMB results for four ambient monitoring sites in the southeastern United States. *Atmospheric environment*, *42*(18), 4126-4137.
- Lewis, C. W., Baumgardner, R. E., Stevens, R. K., Claxton, L. D., & Lewtas, J. (1988). Contribution of woodsmoke and motor vehicle emissions to ambient aerosol mutagenicity. *Environmental Science & Technology*, *22*(8), 968-971.
- Li, C.-S., & Kuo, Y.-M. (1992). Airborne characterization of fungi indoors and outdoors. *Journal of aerosol science*, *23*, 667-670.
- Liao, H.-T., Chou, C. C.-K., Chow, J. C., Watson, J. G., Hopke, P. K., & Wu, C.-F. (2015). Source and risk apportionment of selected VOCs and PM_{2.5} species using partially constrained receptor models with multiple time resolution data. *Environmental Pollution*, *205*, 121-130.
- Liao, H.-T., Kuo, C.-P., Hopke, P. K., & Wu, C.-F. (2013). Evaluation of a modified receptor model for solving multiple time resolution equations: a simulation study. *Aerosol and Air Quality Research*, *13*(4), 1253-1262.
- Liao, H.-T., & Wu, C.-F. (2020). Trajectory-assisted source apportionment of winter-time aerosol using semi-continuous measurements. *Archives of environmental contamination and toxicology*, *78*, 430-438.
- Liao, H.-T., Yau, Y.-C., Huang, C.-S., Chen, N., Chow, J. C., Watson, J. G., Tsai, S.-W., Chou, C. C.-K., & Wu, C.-F. (2017). Source apportionment of urban air pollutants using constrained receptor models with a priori profile information. *Environmental Pollution*, *227*, 323-333.
- Liu, B., Song, N., Dai, Q., Mei, R., Sui, B., Bi, X., & Feng, Y. (2016). Chemical composition and source apportionment of ambient PM_{2.5} during the non-heating period in Taian, China. *Atmospheric Research*, *170*, 23-33.
- Liu, B., Wu, J., Zhang, J., Wang, L., Yang, J., Liang, D., Dai, Q., Bi, X., Feng, Y., &

- 
- Zhang, Y. (2017). Characterization and source apportionment of PM_{2.5} based on error estimation from EPA PMF 5.0 model at a medium city in China. *Environmental Pollution*, 222, 10-22.
- Liu, Y., Zheng, M., Yu, M., Cai, X., Du, H., Li, J., Zhou, T., Yan, C., Wang, X., & Shi, Z. (2019). High-time-resolution source apportionment of PM_{2.5} in Beijing with multiple models. *Atmospheric Chemistry and Physics*, 19(9), 6595-6609.
- Long, Y., Wu, Y., Xie, Y., Huang, L., Wang, W., Liu, X., Zhou, Z., Zhang, Y., Hanaoka, T., & Ju, Y. (2023). PM_{2.5} and ozone pollution-related health challenges in Japan with regards to climate change. *Global Environmental Change*, 79, 102640.
- Mar, T. F., Ito, K., Koenig, J. Q., Larson, T. V., Eatough, D. J., Henry, R. C., Kim, E., Laden, F., Lall, R., & Neas, L. (2006). PM source apportionment and health effects. 3. Investigation of inter-method variations in associations between estimated source contributions of PM_{2.5} and daily mortality in Phoenix, AZ. *Journal of exposure science & environmental epidemiology*, 16(4), 311-320.
- Mimura, T., Ichinose, T., Yamagami, S., Fujishima, H., Kamei, Y., Goto, M., Takada, S., & Matsubara, M. (2014). Airborne particulate matter (PM_{2.5}) and the prevalence of allergic conjunctivitis in Japan. *Science of the Total Environment*, 487, 493-499.
- Norris, G., Duvall, R., Brown, S., & Bai, S. (2014). *EPA positive matrix factorization (PMF) 5.0 fundamentals and user guide*.
- [Record #19 is using a reference type undefined in this output style.]
- Ogulei, D., Hopke, P. K., Zhou, L., Paatero, P., Park, S. S., & Ondov, J. M. (2005). Receptor modeling for multiple time resolved species: the Baltimore supersite. *Atmospheric environment*, 39(20), 3751-3762.
- Omar, N. Y. M., Abas, M. R. B., Rahman, N. A., Tahir, N. M., Rushdi, A. I., & Simoneit, B. R. (2007). Levels and distributions of organic source tracers in air and roadside dust particles of Kuala Lumpur, Malaysia. *Environmental Geology*, 52, 1485-1500.
- Paatero, P., & Hopke, P. K. (2003). Discarding or downweighting high-noise variables in factor analytic models. *Analytica Chimica Acta*, 490(1-2), 277-289.
- Pandis, S. N., Harley, R. A., Cass, G. R., & Seinfeld, J. H. (1992). Secondary organic aerosol formation and transport. *Atmospheric Environment. Part A. General Topics*, 26(13), 2269-2282.
- Puxbaum, H., Caseiro, A., Sánchez-Ochoa, A., Kasper-Giebl, A., Claeys, M., Gelencsér, A., Legrand, M., Preunkert, S., & Pio, C. (2007). Levoglucosan levels at background sites in Europe for assessing the impact of biomass combustion on the European aerosol background. *Journal of Geophysical*



- Research: Atmospheres*, 112(D23).
- Querol, X., Viana, M., Alastuey, A., Amato, F., Moreno, T., Castillo, S., Pey, J., De la Rosa, J., De La Campa, A. S., & Artíñano, B. (2007). Source origin of trace elements in PM from regional background, urban and industrial sites of Spain. *Atmospheric environment*, 41(34), 7219-7231.
- Robinson, A. L., Subramanian, R., Donahue, N. M., Bernardo-Bricker, A., & Rogge, W. F. (2006). Source apportionment of molecular markers and organic aerosol. 3. Food cooking emissions. *Environmental Science & Technology*, 40(24), 7820-7827.
- Rogge, W. F., Hildemann, L. M., Mazurek, M. A., Cass, G. R., & Simoneit, B. R. (1991). Sources of fine organic aerosol. 1. Charbroilers and meat cooking operations. *Environmental Science & Technology*, 25(6), 1112-1125.
- Schauer, J. J., Rogge, W. F., Hildemann, L. M., Mazurek, M. A., Cass, G. R., & Simoneit, B. R. (1996). Source apportionment of airborne particulate matter using organic compounds as tracers. *Atmospheric environment*, 30(22), 3837-3855.
- Shi, G.-L., Tian, Y.-Z., Han, S.-Q., Zhang, Y.-F., Li, X., Feng, Y.-C., Wu, J.-H., & Zhu, T. (2012). Vertical characteristics of carbonaceous species and their source contributions in a Chinese mega city. *Atmospheric environment*, 60, 358-365.
- Shin, S. M., Kim, J. Y., Lee, J. Y., Kim, D.-S., & Kim, Y. P. (2022). Enhancement of modeling performance by including organic markers to the PMF modeling for the PM_{2.5} at Seoul. *Air Quality, Atmosphere & Health*, 15(1), 91-104.
- Simoneit, B. R. (1985). Application of molecular marker analysis to vehicular exhaust for source reconciliations. *International Journal of Environmental Analytical Chemistry*, 22(3-4), 203-232.
- Siudek, P., & Ruczyńska, W. (2021). Simultaneous measurements of PM_{2.5}- and PM₁₀-bound benzo (a) pyrene in a coastal urban atmosphere in Poland: Seasonality of dry deposition fluxes and influence of atmospheric transport. *Aerosol and Air Quality Research*, 21(10), 210044.
- Sofowote, U., Healy, R., Su, Y., Debosz, J., Noble, M., Munoz, A., Jeong, C.-H., Wang, J., Hilker, N., & Evans, G. (2021). Sources, variability and parameterizations of intra-city factors obtained from dispersion-normalized multi-time resolution factor analyses of PM_{2.5} in an urban environment. *Science of the Total Environment*, 761, 143225.
- Song, Y., Tang, X., Xie, S., Zhang, Y., Wei, Y., Zhang, M., Zeng, L., & Lu, S. (2007). Source apportionment of PM_{2.5} in Beijing in 2004. *Journal of hazardous materials*, 146(1-2), 124-130.

- 
- Stanek, L. W., Sacks, J. D., Dutton, S. J., & Dubois, J.-J. B. (2011). Attributing health effects to apportioned components and sources of particulate matter: an evaluation of collective results. *Atmospheric environment*, *45*(32), 5655-5663.
- Tsuang, B.-J., & Chao, J.-P. (1999). Application of circuit model for Taipei City PM10 simulation. *Atmospheric environment*, *33*(11), 1789-1801.
- Urban, R. C., Lima-Souza, M., Caetano-Silva, L., Queiroz, M. E. C., Nogueira, R. F., Allen, A. G., Cardoso, A. A., Held, G., & Campos, M. L. A. (2012). Use of levoglucosan, potassium, and water-soluble organic carbon to characterize the origins of biomass-burning aerosols. *Atmospheric environment*, *61*, 562-569.
- Vallius, M., Janssen, N., Heinrich, J., Hoek, G., Ruuskanen, J., Cyrys, J., Van Grieken, R., De Hartog, J., Kreyling, W., & Pekkanen, J. (2005). Sources and elemental composition of ambient PM_{2.5} in three European cities. *Science of the Total Environment*, *337*(1-3), 147-162.
- Waked, A., Favez, O., Alleman, L., Piot, C., Petit, J.-E., Delaunay, T., Verlinden, E., Golly, B., Besombes, J.-L., & Jaffrezo, J.-L. (2014). Source apportionment of PM₁₀ in a north-western Europe regional urban background site (Lens, France) using positive matrix factorization and including primary biogenic emissions. *Atmospheric Chemistry and Physics*, *14*(7), 3325-3346.
- Walton, N. M., Piketh, S. J., Zyl, P., Maenhaut, W., Burger, R., & Formenti, P. (2021). Source apportionment of ambient fine and coarse aerosols in Embalenhle and Kinross, South Africa. *Clean Air Journal*, *31*(2), 1-13.
- Wang, Q., Shao, M., Zhang, Y., Wei, Y., Hu, M., & Guo, S. (2009). Source apportionment of fine organic aerosols in Beijing. *Atmospheric Chemistry and Physics*, *9*(21), 8573-8585.
- Wang, Y., Zhang, G., & Wang, L. (2015). Potential toxicity of phthalic acid esters plasticizer: interaction of dimethyl phthalate with trypsin in vitro. *Journal of agricultural and food chemistry*, *63*(1), 75-84.
- Wang, Y., Zhuang, G., Tang, A., Yuan, H., Sun, Y., Chen, S., & Zheng, A. (2005). The ion chemistry and the source of PM_{2.5} aerosol in Beijing. *Atmospheric environment*, *39*(21), 3771-3784.
- Watson, J. G. (1984). Overview of receptor model principles. *Journal of the Air Pollution Control Association*, *34*(6), 619-623.
- Watson, J. G., & Chow, J. C. (2001). Source characterization of major emission sources in the Imperial and Mexicali Valleys along the US/Mexico border. *Science of the Total Environment*, *276*(1-3), 33-47.
- Yan, R.-H., Peng, X., Lin, W., He, L.-Y., Wei, F.-H., Tang, M.-X., & Huang, X.-F. (2022). Trends and challenges regarding the source-specific health risk of PM_{2.5}-bound metals in a Chinese megacity from 2014 to 2020.

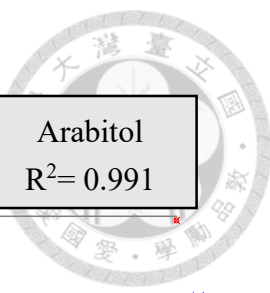


- Environmental Science & Technology*, 56(11), 6996-7005.
- Yatkin, S., Gerboles, M., Belis, C., Karagulian, F., Lagler, F., Barbieri, M., & Borowiak, A. (2020). Representativeness of an air quality monitoring station for PM_{2.5} and source apportionment over a small urban domain. *Atmospheric Pollution Research*, 11(2), 225-233.
- Yen, P.-H., Yuan, C.-S., Ceng, J.-H., Chiang, K.-C., Tseng, Y.-L., Soong, K.-Y., & Jeng, M.-S. (2022). Inter-comparison of chemical fingerprint and source apportionment of marine fine particles at two islands through the west and east passages of the Taiwan Island. *Science of the Total Environment*, 851, 158313.
- Young, L.-H., Li, C.-H., Lin, M.-Y., Hwang, B.-F., Hsu, H.-T., Chen, Y.-C., Jung, C.-R., Chen, K.-C., Cheng, D.-H., & Wang, V.-S. (2016). Field performance of a semi-continuous monitor for ambient PM_{2.5} water-soluble inorganic ions and gases at a suburban site. *Atmospheric environment*, 144, 376-388.
- Yuan, Q., Lai, S., Song, J., Ding, X., Zheng, L., Wang, X., Zhao, Y., Zheng, J., Yue, D., & Zhong, L. (2018). Seasonal cycles of secondary organic aerosol tracers in rural Guangzhou, Southern China: The importance of atmospheric oxidants. *Environmental Pollution*, 240, 884-893.
- Zhou, L., Hopke, P. K., Paatero, P., Ondov, J. M., Pancras, J. P., Pekney, N. J., & Davidson, C. I. (2004). Advanced factor analysis for multiple time resolution aerosol composition data. *Atmospheric environment*, 38(29), 4909-4920.
- 台北市政府環境保護局。(2021)。台北市空氣品質監測報告 110 年年報。
- 李崇德、王家麟、周崇光、張士昱、蕭大智、許文昌 (2018)。107 年度細懸浮微粒(PM_{2.5})化學成分與分析計畫。

Appendixes

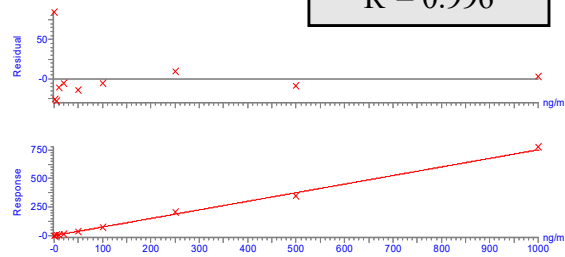
Appendix 1 Calibration curves of 8 organic compounds.....	72
Appendix 2 Sampling dates marked as color blue.....	73
Appendix 3 IS, Matrix spike recovery, LOQ, and MDL of 8 compounds in UPLC-MS/MS analysis	74
Appendix 4 Mass reconstruction exceeding $\pm 40\%$ of measured PM _{2.5} of each month.....	75
Appendix 5 Decisions for double counting deletion.....	76
Appendix 6 The presentation of peaks of 8 compounds in UPLC-MSMS analysis.....	77
Appendix 7 Summary of organic compounds concentrations in other studies	78

Appendix 1 Calibration curves of 8 organic compounds



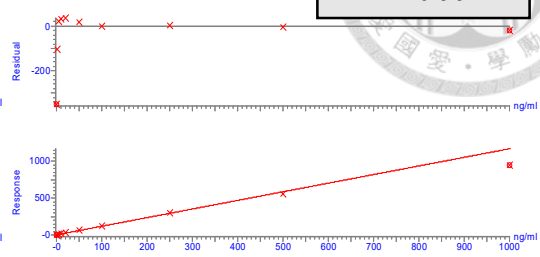
Compound name: Succinic acid
 Correlation coefficient: $r = 0.997583$, $r^2 = 0.995172$
 Calibration curve: $0.749533 \cdot x + 1.36306$
 Response type: Internal Std (Ref 4), Area * (IS Conc. / IS Area)
 Curve type: Linear, Origin: Exclude, Weighting: 1/x, Axis trans: None

Succinic acid
 $R^2 = 0.996$



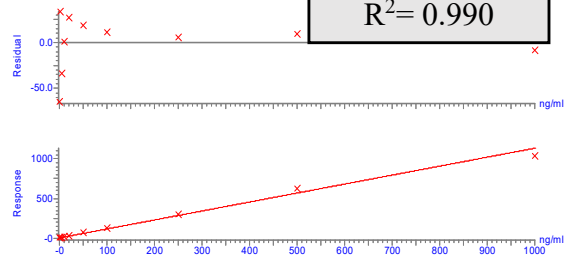
Compound name: Arabitol
 Correlation coefficient: $r = 0.995665$, $r^2 = 0.991349$
 Calibration curve: $1.16883 \cdot x + 2.21337$
 Response type: Internal Std (Ref 3), Area * (IS Conc. / IS Area)
 Curve type: Linear, Origin: Exclude, Weighting: 1/x, Axis trans: None

Arabitol
 $R^2 = 0.991$



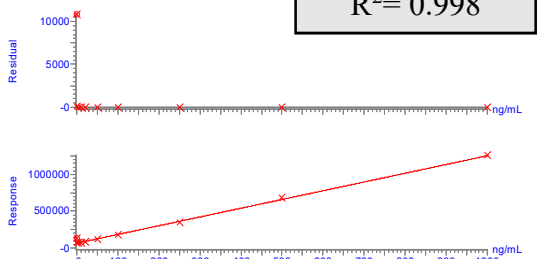
Compound name: Mannitol
 Correlation coefficient: $r = 0.995347$, $r^2 = 0.990716$
 Calibration curve: $1.1259 \cdot x + 5.87844$
 Response type: Internal Std (Ref 3), Area * (IS Conc. / IS Area)
 Curve type: Linear, Origin: Exclude, Weighting: 1/x, Axis trans: None

Mannitol
 $R^2 = 0.990$



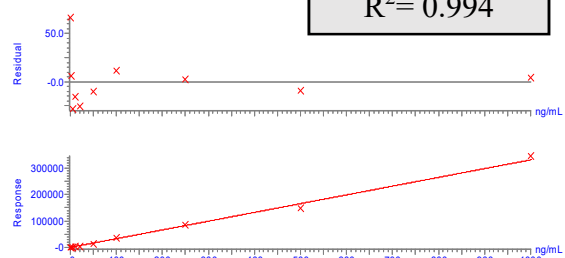
Compound name: Cholesterol
 Correlation coefficient: $r = 0.999099$, $r^2 = 0.998200$
 Calibration curve: $1189.27 \cdot x + 65501.9$
 Response type: External Std, Area
 Curve type: Linear, Origin: Exclude, Weighting: 1/x, Axis trans: None

Cholesterol
 $R^2 = 0.998$



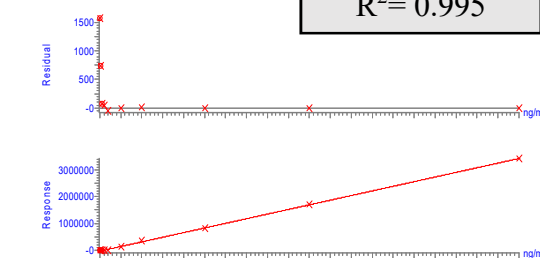
Compound name: 2-Methylerythritol
 Correlation coefficient: $r = 0.997176$, $r^2 = 0.994359$
 Calibration curve: $331.85 \cdot x - 169.398$
 Response type: External Std, Area
 Curve type: Linear, Origin: Exclude, Weighting: 1/x, Axis trans: None

2-MT
 $R^2 = 0.994$



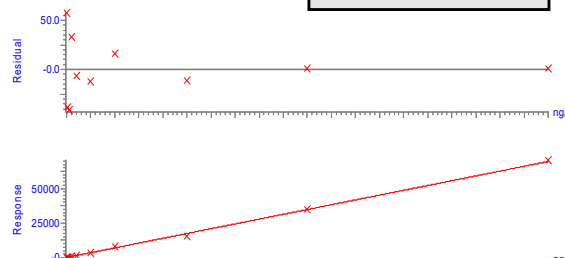
Compound name: 2,3-dihydroxy-4-oxopentanoic acid
 Correlation coefficient: $r = 0.997572$, $r^2 = 0.995150$
 Calibration curve: $3448.27 \cdot x + 28876.5$
 Response type: External Std, Area
 Curve type: Linear, Origin: Exclude, Weighting: 1/x, Axis trans: None

DHOPA
 $R^2 = 0.995$



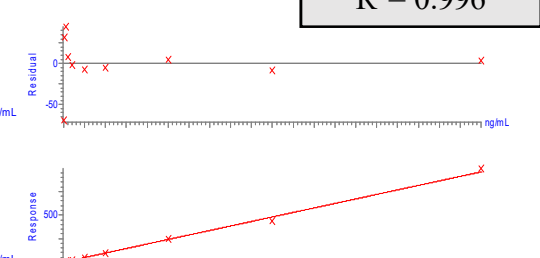
Compound name: Levoglucosan
 Correlation coefficient: $r = 0.997711$, $r^2 = 0.995427$
 Calibration curve: $69.6096 \cdot x + 23.7494$
 Response type: External Std, Area
 Curve type: Linear, Origin: Exclude, Weighting: 1/x, Axis trans: None

Levoglucosan
 $R^2 = 0.995$



Compound name: Phthalic acid
 Correlation coefficient: $r = 0.998115$, $r^2 = 0.996233$
 Calibration curve: $0.959153 \cdot x + 0.870095$
 Response type: Internal Std (Ref 11), Area * (IS Conc. / IS Area)
 Curve type: Linear, Origin: Exclude, Weighting: 1/x, Axis trans: None

Phthalic acid
 $R^2 = 0.996$



Appendix 2 Sampling dates marked as color blue



October 2022
Sun/10/29/11/12/13/14/15/16/17/18/19/20/21/22/23/24/25/26/27/28/29/30/31

NOVEMBER 2022

Sunday	Monday	Tuesday	Wednesday	Thursday	Friday	Saturday
		1	2	3	4	5
6	7	8	9	10	11	12
13	14	15	16	17	18	19
20	21	22	23	24	25	26
27	28	29	30			

12/1/2022 10:56:12 AM

December 2022
Sun/12/4/5/6/7/8/9/10/11/12/13/14/15/16/17/18/19/20/21/22/23/24/25/26/27/28/29/30/31

DECEMBER 2022

Sunday	Monday	Tuesday	Wednesday	Thursday	Friday	Saturday
				1	2	3
4	5	6	7	8	9	10
11	12	13	14	15	16	17
18	19	20	21	22	23	24
25	26	27	28	29	30	31

12/1/2022 10:56:12 AM

December 2022
Sun/12/4/5/6/7/8/9/10/11/12/13/14/15/16/17/18/19/20/21/22/23/24/25/26/27/28/29/30/31

JANUARY 2023

Sunday	Monday	Tuesday	Wednesday	Thursday	Friday	Saturday
1	2	3	4	5	6	7
8	9	10	11	12	13	14
15	16	17	18	19	20	21
22	23	24	25	26	27	28
29	30	31				

12/1/2022 10:56:12 AM

January 2023
Sun/1/1/2/3/4/5/6/7/8/9/10/11/12/13/14/15/16/17/18/19/20/21/22/23/24/25/26/27/28/29/30/31

FEBRUARY 2023

Sunday	Monday	Tuesday	Wednesday	Thursday	Friday	Saturday
			1	2	3	4
5	6	7	8	9	10	11
12	13	14	15	16	17	18
19	20	21	22	23	24	25
26	27	28				

12/1/2022 10:56:12 AM

February 2023
Sun/2/1/2/3/4/5/6/7/8/9/10/11/12/13/14/15/16/17/18/19/20/21/22/23/24/25/26/27/28/29/30

MARCH 2023

Sunday	Monday	Tuesday	Wednesday	Thursday	Friday	Saturday
			1	2	3	4
5	6	7	8	9	10	11
12	13	14	15	16	17	18
19	20	21	22	23	24	25
26	27	28	29	30	31	

12/1/2022 10:56:12 AM

March 2023
Sun/3/1/2/3/4/5/6/7/8/9/10/11/12/13/14/15/16/17/18/19/20/21/22/23/24/25/26/27/28/29/30/31

APRIL 2023

Sunday	Monday	Tuesday	Wednesday	Thursday	Friday	Saturday
						1
2	3	4	5	6	7	8
9	10	11	12	13	14	15
16	17	18	19	20	21	22
23	24	25	26	27	28	29
30						

12/1/2022 10:56:12 AM

Appendix 3 IS, Matrix spike recovery rate, and MDL of 8 compounds in UPLC-MS/MS analysis

Compounds	IS	Recovery rate (%)	MDL (ng/mL)
2-MT	Meso-erythritol-D ₆	95-109	1.54
DHOPA	(Quantified by external calibration)	96-105	0.57
Levoglucosan	Levoglucosan-d ₇	96-107	1.68
Phthalic acid	Phthalic acid-d ₄	93-110	5.95
Succinic acid	Succinic acid-d ₄	84-92	0.87
Arabitol	D-Mannitol-13C	101-119	0.65
Mannitol		93-117	0.86
Cholesterol	Cholesterol-13C	85-119	0.01

Appendix 4 Mass reconstruction exceeding $\pm 40\%$ of measured PM_{2.5} of each month

month	8	9	10	11	12	1	3	4
missing	13%	9%	11%	23%	25%	11%	9%	20%
Percent of exceeding $\pm 40\%$	29%	39%	28%	52%	6%	28%	26%	28%

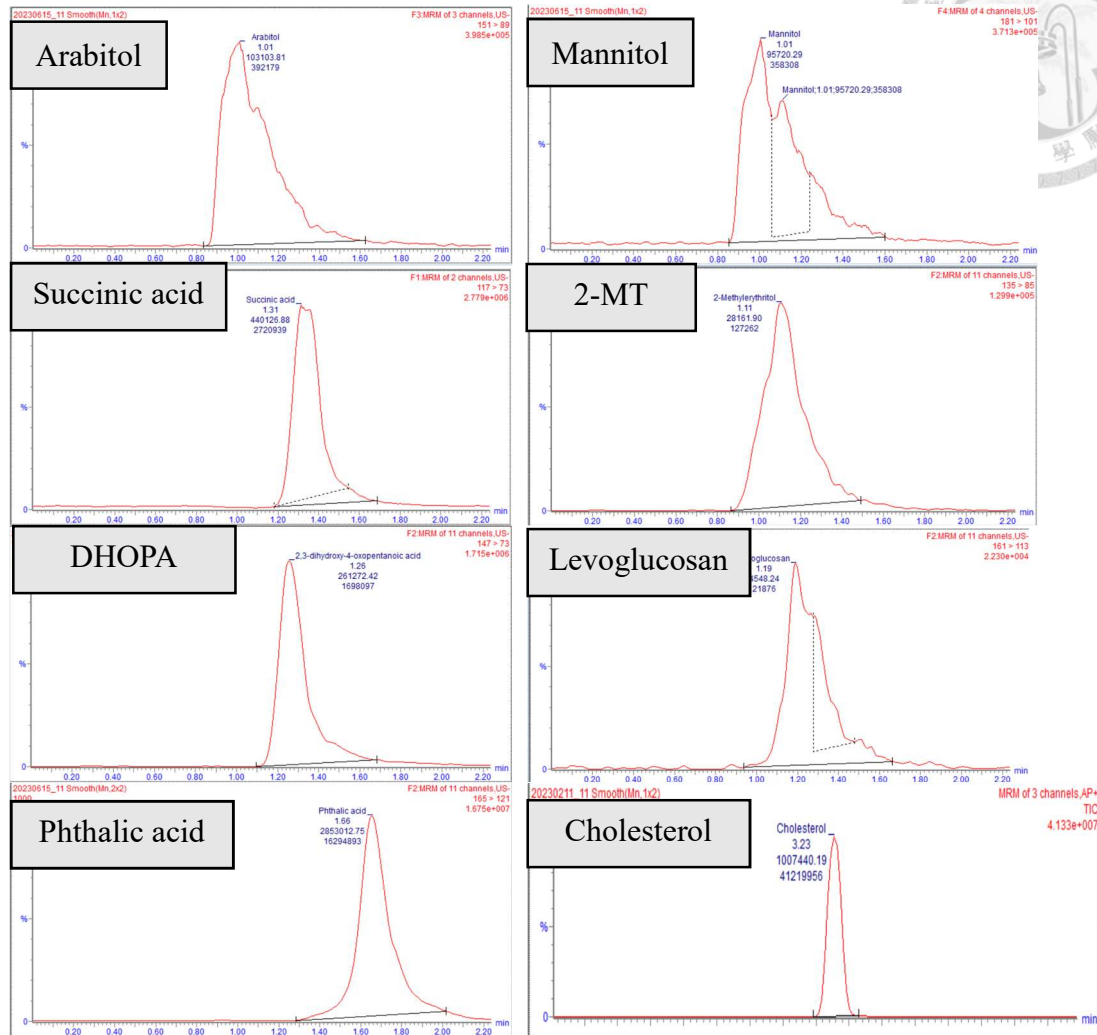
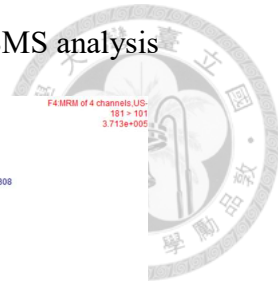
Appendix 5 Decisions for double counting deletion

	Cl	Cl ⁻	S	SO ₄ ²⁻	K	K ⁺	Ca	Ca ₂ ⁺
S/N	7.83	5.6	8.24	7.11	8.17	1.21	8.48	5.88
BDL	124	189	83	185	67	810	63	178
	excluded	Important marker for sea salt	excluded	Important marker for secondary aerosols		excluded		excluded

S/N: Signal-to-noise ratio (S/N) is a parameter for qualities of species.

BDL: the number of below detection limit

Appendix 6 The presentation of peaks of 8 compounds in UPLC-MSMS analysis



Appendix 7 Summary of organic compounds concentrations in other studies

Compounds	Reference	Concentration (ng/m ³)		
		mean	minimum	maximum
Arabitol	This study	2.27	ND	19.82
	L. Liang et al, 2016	7.4	0.7	-
	Gehui Wang et al, 2011	-	16.0	-
Mannitol	This study	8.88	ND	76.26
	L. Liang et al, 2016	10.3	0.9	-
	Gehui Wang et al, 2011	-	24.0	-
	Mengxin Xiao, 2018	25.3	3.0	138.0
Succinic acid	This study	36.11	10.6	85.43
	Gehui Wang et al, 2011	-	50.0	-
	Monica Ivone A.M et al., 2020	77.0	48.4	-
2-MT	This study	0.61	ND	4.91
	Mengxin Xiao, 2018	13.8	1.6	-
Levoglucosan	This study	16.98	4.11	69.35
	Gehui Wang et al, 2011	689.0	75.0	-
	Monica Ivone A.M et al., 2020	354.0	140.9	-
	L. Liang et al, 2016	369.2	23.7	-
DHOPA	This study	1.80	ND	9.06
	Rui Li et al, 2020	3.9	-	-
phthalic acid	This study	13.66	2.10	62.08
	Gehui Wang et al, 2011	60.8	16.4	-

- means not mentioned in the study